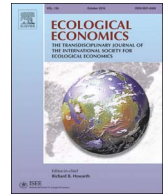




Contents lists available at ScienceDirect

## Ecological Economics

journal homepage: [www.elsevier.com/locate/ecocon](http://www.elsevier.com/locate/ecocon)

## Analysis

## Coping With Collapse: A Stock-Flow Consistent Monetary Macrodynamics of Global Warming

Emmanuel Bovari<sup>b,c</sup>, Gaël Giraud<sup>a,b,c</sup>, Florent Mc Isaac<sup>a,c,\*</sup><sup>a</sup> Agence Française de Développement (AFD), 5 Rue Roland-Barthes, Paris 75012, France<sup>b</sup> Centre d'Économie de la Sorbonne, Paris 1 University Panthéon-Sorbonne, 106-112 bd. de l'Hôpital, Paris 75013, France<sup>c</sup> Chair Energy & Prosperity, Institut Louis Bachelier, 28 place de la Bourse, 75002 Paris, France

## ARTICLE INFO

## JEL Classification:

C51  
D72  
E12  
O13  
Q51  
Q54

## Keywords:

Ecological macroeconomics  
Stock-flow consistent model  
Climate change  
Integrated assessment  
Collapse  
Debt

## ABSTRACT

This paper presents a macroeconomic model that combines the economic impact of climate change with the pivotal role of private debt. Using a Stock-Flow Consistent approach based on the Lotka–Volterra logic, we couple its nonlinear monetary dynamics of underemployment and income distribution with abatement costs. A calibration of our model at the scale of the world economy enables us to simulate various planetary scenarios. Our findings are threefold: 1) the +2 °C target is already out of reach, absent negative emissions; 2) the long-term (resp. short-term) results of climate change on economic fundamentals may lead to severe economic consequences without the implementation (resp. in case of too rapid an application) of proactive climate policies. Global warming (resp. too fast transition) forces the private sector to leverage in order to compensate for output and capital losses (resp. to lower carbon emissions), thus endangering financial stability; 3) Implementing an adequate carbon price trajectory, as well as increasing the wage share, fostering employment, and reducing private debt make it easier to avoid unintended degrowth and to reach a +2.5 °C target.

## 1. Introduction

Given the increasing awareness of climate disturbance, which crystallized at a diplomatic level in the Paris Agreement of December 2015, and the growing concern about potential downside consequences of a temperature increase, the question is raised of whether global warming might *per se* destabilize the world economy. This paper contributes to this issue and sheds some light on one way to avoid this threat by relying on a carbon price mechanism set by the regulator. More particularly, according to the Paris Agreement, 195 countries pledged to reach net zero emissions in the second half of this century.

Yet, beyond the bio-physical issue of warming, the financial stake of the cost of mitigation and adaptation should not be neglected either. According to the [New Climate Economy Report \(2014\)](#), US\$ 90 trillion are needed at the world level over the next 15 years to fund clean infrastructure that would make it possible to reach zero net emissions, which prompts a pressing question: how will the world economy fi-

nance such monetary flows? Given today's vulnerability of public finances, it is expected that the private sector will be able to endorse the much needed long-run investments. This, in turn, raises a new question: will the world economy be able to carry the corresponding additional private debt burden?<sup>1</sup> As argued by Bank of England Governor Mark Carney ([Carney, 2016](#)), too rapid a movement towards a low-carbon economy could materially damage financial stability.

Taking advantage of a growing body of literature in ecological macroeconomics —see, for instance, [Barrett \(2018\)](#), [Dafermos et al. \(2017\)](#), [Dietz and Stern \(2015\)](#), [Jackson \(2009\)](#), [Nordhaus and Storz \(2013\)](#), [Rezai and Stiglitz \(2016\)](#), [Rezai et al. \(2018, 2013\)](#)—, we present an integrated ecological macroeconomic model that combines two sources of instability: (i) global warming and (ii) private over-indebtedness. By incorporating the latter into a rather low-dimensional stock-flow consistent integrated assessment model (hereafter IAM), we are able to track transmission channels between the two sources of potential economic vulnerability alluded to by Carney. As already made

\* Corresponding author at: Agence Française de Développement (AFD), 5 Rue Roland-Barthes, Paris 75012, France.

E-mail address: [mcisaacf@afd.fr](mailto:mcisaacf@afd.fr) (F. Mc Isaac).

<sup>1</sup> See [Giraud \(2017\)](#) for a first grasp of this issue.

clear by Nordhaus (2016) among others, the +2 ° C target seems already to be out of reach absent carbon sequestration. That is why we discuss carbon pricing trajectories that succeed in avoiding a severe recession by implementing a feasible cap on global warming that does not necessarily remain below +2 ° C.

The paper is organized as follows. Section 2 briefly links our stock-flow consistent model with the background literature on IAMs. Section 3 sets up the modeling framework. Section 4 provides some first mathematical insights into the destabilizing impact of climate change on our modeling. Section 5 addresses this interplay more extensively and numerically through an analysis of three prospective scenarios. Section 6 discusses the deployment of a public policy instrument—a carbon price—that may help cope with the possible climate and financial disasters that emerge from the analysis in the previous sections. Our main conclusions and areas for future research are outlined in the final section.

## 2. Alternative Modeling Foundations

Over the past thirty years, many IAMs have been developed to estimate the impact of economic development on the environment. A solid body of literature compares IAMs, describing their advantages and disadvantages, e.g., Schwanitz (2013). The models considered in this literature usually involve macroeconomic settings that rely on welfare maximization, general equilibrium, partial equilibrium and cost minimization (Stanton et al., 2009). For instance, the core economic model of the DICE model of Nordhaus (1993), the benchmark for IAM literature, is the Ramsey–Cass–Koopmans approach. It assumes a closed economy endowed with a constant return to scale Cobb–Douglas technology combining labor and capital, where agents' decisions are made under perfect foresight. At the steady state, output increases at the pace of labor force growth and technological progress while factor costs adjust such that all markets clear. By construction, such a dynamics precludes situations such as mass unemployment and over-indebtedness.

By contrast, recent research has contributed to building alternatives to such IAMs by incorporating Keynesian features (see, e.g., Barker et al., 2012) or more post-Keynesian insights (see, e.g. Dafermos et al., 2017). Our modeling approach does not assume fully optimal behavior either. Instead, it relies on the ideas of Hyman Minsky on the intrinsic instability of a monetary market economy, which have experienced a significant revival in the aftermath of the 2007–2009 financial crisis. We adopt a mathematical formalization of Minsky's standpoint to assess the role of private debt dynamics in our narrative.<sup>2</sup> Our starting point is the prey-predatory macrodynamics first introduced by Goodwin (1967) and Akerlof and Stiglitz (1969), and later extended by Keen (1995). Building on this insight, we offer a model based on the myopic behavior of imperfectly competitive firms, which is stock-flow consistent (Godley and Lavoie, 2012), allows for multiple long-run equilibria, and exhibits endogenous monetary cycles, sticky prices, endogenously determined private debt, and underemployment. Moreover, money is endogenously created by the banking sector (Giraud and Grasselli, 2017). Here, by contrast with more conventional general equilibrium approaches, the current state of the economy may be already following a path leading to a future severe economic recession if no shift away from a business-as-usual scenario is implemented.<sup>3</sup>

<sup>2</sup> Dos Santos (2005) provides a survey up to 2005 of the literature on the modeling of Minskian instability; more recent contributions include Ryoo (2010) and Chiarella and Di Guilmi (2011).

<sup>3</sup> Dietz and Stern's (2015) extension shows that the DICE model can also exhibit output trajectories characterized by a severe economic recession, as does the model introduced in this paper. In addition, however, we characterize such recessive paths in terms of mass unemployment and private over-indebtedness — which are difficult to obtain in the DICE equilibrium model.

## 3. An Integrated Framework

Our IAM depicts the interrelations between a global monetary economy and climate change. Although, for simplicity, the public sector is not explicitly modeled, public policy objectives are materialized through the deployment of a carbon price that allows a decentralized emission reduction rate to be achieved.<sup>4</sup> The core macroeconomic module is presented in Subsection 3.1 and the climate module is detailed in Subsection 3.2. The introduction of damages and the way these can be controlled through public policy objectives is discussed in Subsection 3.3. The empirical calibration of the IAM is provided in Appendix E.

### 3.1. The Monetary Macrodynamics

Our macroeconomic model belongs to the literature centered around Keen (1995).<sup>5</sup> One appeal of this framework lies in its ability to formalize long-term economic deflation and degrowth as a consequence of over-indebtedness.

#### 3.1.1. Damaged Production and Abatement

The productive sector produces a real amount,  $Y^0$ , of a unique consumption good combining labor and capital:

$$Y^0 = \frac{K}{\nu} = aL, \quad (1)$$

where  $K$  and  $L$  refer respectively to the stock of capital and labor, while  $\nu$  and  $a$  stand respectively for the (constant) capital–output ratio and Harrod-neutral labor-augmenting technological level. For simplicity, full capital use is assumed and Say's law is postulated.

As defined shortly, economic activities release CO<sub>2</sub>-e emissions that will be priced through a carbon pricing instrument (carbon tax). As an answer to the tax burden, the productive sector may engage in abatement activities to lower its CO<sub>2</sub>-e emissions. By doing so, a fraction,  $A$ , of output,  $Y^0$ , is diverted from its final use, and serves instead as an intermediate consumption in order to reduce CO<sub>2</sub>-e emissions as defined shortly. Moreover, as in Nordhaus (2007), a proportion  $D^Y$  of the remaining output is damaged beyond repair by global warming and lost. Consequently, the production available on the commodity market is given by

$$Y = (1 - D^Y)(1 - A)Y^0. \quad (2)$$

#### 3.1.2. Profits, Investment and Inflation

Let us denote by  $p$  the consumption price,  $\Pi$ , the nominal net profit,  $w$ , the unitary money wage,  $r$ , the short-term interest rate<sup>6</sup>,  $L_c$ , the total amount of corporate debt,  $M_c$ , the deposits held by the productive sector,  $p_c$ , the real price of a ton of CO<sub>2</sub>-e expressed in 2010 US\$,  $E_{ind}$ , the volume of industrial emissions in GtC, to be defined shortly, and  $\delta > 0$  the standard depreciation rate of capital. Nominal profit,  $\Pi$ , is defined as the nominal output minus production cost:

$$\Pi = pY - wL - rD - pT_f - p\delta_D K. \quad (3)$$

The cost of production is the sum of: (i) the wage bill,  $wL$ ; (ii) the private debt burden—where  $D := L_c - M_c$  stands for the outstanding balance of current nominal private debt; (iii) the payment of the carbon tax,  $pT_f := pp_c E_{ind}$ ; and (iv) the global depreciation rate of capital,  $\delta_D := \delta + D^K$ , where  $D^K$  is the rate of degradation induced by climate

<sup>4</sup> Public intervention, as well as the resulting dynamics of public debt are left for future research.

<sup>5</sup> Such as Grasselli and Lima (2012), Grasselli et al. (2014), Nguyen-Huu and Costa-Lima (2014), Grasselli and Nguyen-Huu (2015b) and Giraud and Grasselli (2017) *inter alia*.

<sup>6</sup> For simplicity,  $r$  is kept constant here. Endogenous short-run interest rate is left for future research.

change, defined shortly. Defining both the money wage share,  $\omega$ , and the private debt ratio,  $d$ , by Eq. (4), the nominal profit share,  $\pi$ , can now be expressed by Eq. (5):

$$\omega := \frac{wL}{pY} \quad \text{and} \quad d := \frac{D}{pY}, \tag{4}$$

$$\pi := \frac{\Pi}{pY}. \tag{5}$$

Real investment,  $I$ , is assumed to be driven by the profit share,  $\pi$ , capturing the risk apptence of the corporate sector. This leads to the following capital accumulation equation expressed in real terms:

$$I := \kappa(\pi)Y, \tag{6}$$

$$\dot{K} := I - \delta_D K, \tag{7}$$

where  $\kappa(\cdot)$  is an increasing, smooth real-valued function. The behavior of the productive sector incorporates the current level of climate damages inasmuch as investment decisions depend upon the output net of environmental damages,  $Y$ , entering into Eq. (5). For our empirical applications, the function,  $\kappa(\cdot)$ , introduced in Eq. (6), will be calibrated.<sup>7</sup>

Changes in nominal private corporate debt,  $D$ , depend on the gap between current nominal profit,  $\Pi$ , and nominal investment,  $pI$ , plus nominal dividends paid to shareholders,  $\Pi_d(\pi)$ :

$$\dot{D} := pI + \Pi_d(\pi) - \Pi - p\delta_D K, \tag{8}$$

$$\Pi_d(\pi) := \Delta(\pi)pY. \tag{9}$$

According to Eq. (9), the current level of nominal dividends, viewed as a fraction of nominal output is assumed to be an increasing real-valued function,  $\Delta(\cdot)$ , of the profit share,  $\pi$ .<sup>8</sup> The resulting retained profits  $\Pi_r := \Pi - \Pi_d$  are used to finance various expenses as outlined in the stock-flow Table 1. Eq. (8) implies that some corporates might borrow money to finance dividends. This should not come as a surprise as it is consistent with the celebrated Modigliani–Miller theorem (Hellwig, 1981), which states that both equity and debt are equivalent ways to finance a corporate's expenditures. Thus, Eq. (8) may be interpreted as meaning, at least implicitly, that firms behave as if they believed the Modigliani–Miller theorem to be true. Moreover, contemporary oil companies are known to issue debt in order to pay their shareholders (Nasdaq.com, 2016).

Both the profits from the banking sector,  $rD$ , and the carbon tax,  $pT_f$ , paid by the productive sector are redistributed to the shareholders either as dividends or as a lump-sum transfer. Thus, the whole income that accrues to households is  $wL + \Pi_d + rD + pT_f$ . As a consequence, abatement costs are transmitted to households via dividends paid to shareholders: *ceteris paribus*, abatement costs reduce profits, which reduces dividends.

Finally, Eq. (10) captures the dynamics of inflation: the consumption price,  $p$ , converges to its long-run equilibrium value through a lagged adjustment of exponential form with a relaxation time,  $1/\eta_p$ .<sup>9</sup> The long-run equilibrium price is given by a markup,  $m \geq 1$ <sup>10</sup>, times the average unitary cost of production,  $c$ :

$$i := \frac{\dot{p}}{p} := \eta_p (mc - 1), \tag{10}$$

$$c := \frac{1}{(1-A)(1-D^Y)} \left[ \frac{w}{pa} + \nu(\text{WACC} + \delta_D) + p_c \sigma (1-n) \right]. \tag{11}$$

<sup>7</sup> More details on our calibration are available in Appendix E and our method in Appendix C.

<sup>8</sup> In our empirical applications, the aggregate behavioral functions,  $\kappa(\cdot)$  and  $\phi(\cdot)$ , have been bounded to avoid inconsistent behaviors that might fall far outside the estimation range. See Nguyen-Huu and Pottier (2016) for a methodological discussion of this point.

<sup>9</sup> The parameter  $\eta_p$  captures the viscosity of prices, hence it plays a role analogous to the Calvo parameter in the neo-Keynesian literature, cf. e.g., Calvo (1983).

<sup>10</sup> Whenever the consumption goods market is imperfectly competitive,  $m > 1$ .

The cost of production,  $c$ , encapsulates respectively the cost of labor, the cost of capital, and the cost of carbon emission. The WACC (weighted average cost of capital) is defined as the cost of debt services plus dividends, i.e.,  $\text{WACC} := (rD + \Delta(\pi)pY)/pK$ . The parameter,  $n$ , and  $\sigma$ , refer to the emission reduction rate, and the current emission intensity, both defined in the next section. Clearly, this dynamics of inflation (to be calibrated in the sequel) presumes that the productive sector partly charges the cost of emitting CO<sub>2</sub>-e to its clients.

### 3.1.3. The Labor Market

The world workforce,  $N$ , is assumed to grow according to a sigmoid inferred from the 15–64 age group in the United Nations (2015) median scenario:

$$\beta(N) := \frac{\dot{N}}{N} = q \left( 1 - \frac{N}{P^N} \right), \tag{12}$$

where  $P^N$  stands for the upper bound of the world's labor force and  $q$  for the speed of convergence towards  $P^N$ .<sup>11</sup> The employment rate is defined in Eq. (13) as the ratio between the number of employed workers,  $L$ , and the global labor force,  $N$ :<sup>12</sup>

$$\lambda := \frac{L}{N}. \tag{13}$$

The link between the real and nominal spheres of the economy is provided by short-run wage-price dynamics taken from Grasselli and Nguyen Huu (2018).<sup>13</sup>

$$\frac{\dot{w}}{w} := \phi(\lambda). \tag{14}$$

In other words, workers bargain for their wages,  $w$ , based on the current state of employment,  $\lambda$ , through some increasing real-valued function,  $\phi(\cdot)$ , which will be calibrated.

Finally, the behavior of households is fully accommodating in the sense that, given investment and output, consumption is pinned down by the macro balance:  $C := Y - I$ .

### 3.2. The Climate Module

Our formalization of the emissions and climate anomaly closely follows the conventional framework introduced by Nordhaus in his seminal work, for instance Nordhaus (1993) or Nordhaus (2014), for the DICE model, adapted here to our continuous time framework.

$$E := E_{ind} + E_{land}. \tag{15}$$

$$E_{ind} := Y^0 \sigma (1 - n), \tag{16}$$

$$\frac{\dot{\sigma}}{\sigma} := g_\sigma, \tag{17}$$

$$\frac{g_\sigma}{g_\sigma} := \delta_{g_\sigma}, \tag{18}$$

$$\frac{\dot{E}_{land}}{E_{land}} := \delta_{E_{land}}. \tag{19}$$

As shown by Eqs. (15)–(19), global CO<sub>2</sub>-e emissions are the sum of: (i) industrial emissions,  $E_{ind}$ , linked to real produced output and (ii) land-use emissions,  $E_{land}$ .<sup>14</sup> The latter source of emissions is exogenous

<sup>11</sup> The details of the calibration of these parameters can be given upon request.

<sup>12</sup> The constraint  $L \leq N$  is assumed to be never binding. Indeed, because of some irreducible frictional residual of temporary underemployment, “full employment” usually means that about 95% or so of the working population is hired. On the other hand, mass unemployment or part time labor in the Old World—and similarly, informal labor in Southern countries—make it hard to imagine economies where aggregate labor demand would be rationed.

<sup>13</sup> See also Mankiw (2010).

<sup>14</sup> This second contribution can be viewed as being induced by deforestation and the implied release of CO<sub>2</sub>-e.

and decreases at rate  $\delta_{E_{land}} < 0$ . The level of industrial emissions defined in Eq. (16) depends on the current emission intensity of the economy,  $\sigma$ ,<sup>15</sup> mitigation efforts captured through the emission-reduction rate,  $n$ , defined shortly, and the output level of the economy.

$$\begin{pmatrix} \dot{CO}_2^{AT} \\ \dot{CO}_2^{UP} \\ \dot{CO}_2^{LO} \end{pmatrix} = \begin{pmatrix} E \\ 0 \\ 0 \end{pmatrix} + \Phi \begin{pmatrix} CO_2^{AT} \\ CO_2^{UP} \\ CO_2^{LO} \end{pmatrix}, \tag{20}$$

where:

$$\Phi = \begin{pmatrix} -\phi_{12} & \phi_{12} C_{UP}^{AT} & 0 \\ \phi_{12} & -\phi_{12} C_{UP}^{AT} - \phi_{23} & \phi_{23} C_{LO}^{UP} \\ 0 & \phi_{23} & -\phi_{23} C_{LO}^{UP} \end{pmatrix} \tag{21}$$

$$C_i^j = \frac{C_{j_{pind}}}{C_{i_{pind}}}, (i, j) \in \{AT, UP, LO\}^2, \tag{22}$$

The carbon cycle is represented in Eqs. (20)–(22) through an interacting three-layer model in which global CO<sub>2</sub>-e emissions,  $E$ , accumulate, including: (i) the atmosphere (AT); (ii) a mixing reservoir in the upper ocean and the biosphere (UP); and (iii) the deep ocean (LO). When the level of emissions disappears following completion of the energy shift, the total amount of CO<sub>2</sub>-e (existing and released) will spread according to the diffusion parameters  $\Phi_{ij}, (i, j) \in \{1, 2, 3\}^2$ , such that the relative preindustrial concentrations  $C_{i_{pind}}, i \in \{AT, UP, LO\}$  in each layer are respected at equilibrium.

$$F = F_{ind} + F_{exo}, \tag{23}$$

$$F_{ind} = \frac{F_{2 \times CO_2}}{\log(2)} \log\left(\frac{CO_2^{AT}}{C_{AT_{pind}}}\right), \tag{24}$$

The accumulation of greenhouse gases modifies the chemical properties and thus the energy balance of the atmosphere layer, triggering a rise in the radiative forcing,  $F$ , of CO<sub>2</sub>-e as modeled by Eqs. (23)–(24). A distinction is made between industrial forcing,  $F_{ind}$  (from CO<sub>2</sub>-e) and residual forcing,  $F_{exo}$ .<sup>16</sup> Note that in Eq. (24), the parameter  $F_{2 \times CO_2}$  represents the increase in the radiative forcing resulting from a doubling of the preindustrial CO<sub>2</sub>-e concentration.

$$C\dot{T} = F - \rho T - \gamma^*(T - T_0), \tag{25}$$

$$C_0 \dot{T}_0 = \gamma^*(T - T_0). \tag{26}$$

Eventually, the rise in radiative forcing induces a change,  $T$ , in the global mean atmospheric temperature, as follows from Eqs. (25)–(26). The global thermal behavior results from a coupled two-layer energy-balance model that roughly represents: (i) the atmosphere, land surface, and upper ocean with a mean temperature,  $T$ , and (ii) the deeper ocean with a mean temperature,  $T_0$ . In this framework, the latter layer encapsulates the long-run thermal inertia effects of the climate system. The remaining parameters are:  $\rho$ , the radiative feedback parameter;  $\gamma^*$ , the heat exchange coefficient between the two layers;  $C$ , the heat capacity of the atmosphere, land surface, and upper ocean layer; and  $C_0$ , the heat capacity of the deep ocean layer. As Geoffroy et al. (2013) pointed out, this formalism enables us to account for the two-frequency responses of the mean atmospheric temperature change through a distinct transient climate response (TCR) and an equilibrium climate sensitivity (ECS, determined by  $T = F/\rho$  in this framework).<sup>17</sup>

<sup>15</sup> The dynamics of  $\sigma$  is given by Eqs. (17) and (18), where  $\delta_{\sigma} < 0$  is a parameter

<sup>16</sup> The residual forcing results from various residual factors such as non-CO<sub>2</sub>-e long-lived greenhouse gases and other factors such as albedo changes, or the cloud effect. For simplicity, it is taken here as exogenous, as IPCC (2013) showed it to be negligible and in line with representative concentration pathways. To do so, we rely on the formalization of Nordhaus (2016) with a linear trajectory up to 2100, followed by a plateau.

<sup>17</sup> TCR and ECS represent the mean atmospheric temperature deviations, at different

### 3.3. Damages and Mitigation

We couple the macroeconomic and climate modules in a way similar to Nordhaus (2014), that is, through: (i) an environmental damage function that quantifies the real economic loss due to global warming and (ii) mitigation efforts implemented through the deployment of a carbon price instrument. Finally, achieving the energy shift will impose a carbon abatement cost, already introduced above.

#### 3.3.1. Environmental Damages

The damage function summarizes the total economic impacts brought on by the rise in mean atmospheric temperature. It thus has to compile a wide range of events, including biodiversity loss, ocean acidification, sea level rise, change in ocean circulation, and highly frequent storms, among others, and consequently exhibits highly non-linear and threshold effects. Conventional damage functions, as introduced by Nordhaus in his seminal work Nordhaus and Sztorc (2013), are designed to express the aggregate economic impact of climate change as a fraction of current real output. However, as rightly pointed out by Dietz and Stern (2015) and Dafermos et al. (2017), global warming may have an adverse impact not only on output but also on the factors of production themselves, such as the capital stock. To capture the total amount of damages,  $D$ , on the economy, and the way it distributes between output,  $D^Y$ , and the stock of capital,  $D^K$ , we borrow the functional form and calibration provided by Dietz and Stern (2015) with a polynomial damage function as described in Eq. (27)

$$D = 1 - \frac{1}{1 + \pi_1 T + \pi_2 T^2 + \pi_3 T^3}, \tag{27}$$

$$D^K = f_K D, \tag{28}$$

$$D^Y = 1 - \frac{1 - D}{1 - D^K}, \tag{29}$$

where  $f_K \in [0, 1]$  quantifies the fraction of damages borne by the capital stock. The allocation rule given in Eqs. (28)–(29) ensures that the instantaneous level of damages on real output is identical to the one introduced by Dietz and Stern (2015). In the medium run, however, our specification will have more severe effects since the potential output of the economy, driven by the current stock of capital, is now penalized.

#### 3.3.2. Abatement Efforts and Reduction of Emissions

Carbon emission abatement is achieved at some cost, which is borne by the productive sector as an intermediary consumption. A fraction of real output,  $A$ , is diverted from sales in order to reduce the burden of the carbon tax, which is calculated upon the total level of industrial CO<sub>2</sub>-e emissions. Depending on the level of carbon price, the productive sector endogenously chooses its emission reduction rate,  $n \geq 0$ , which depends on the absolute value of the carbon tax, as well as on the abatement technology,  $A$ . The latter involves the emission intensity,  $\sigma$ ,<sup>18</sup> and the price of the backstop technology,  $p_{BS}$ :

$$A = \frac{\sigma p_{BS}}{\theta} n^\theta, \tag{30}$$

where the parameter  $\theta$  controls the convexity of the cost.

The resulting emission reduction rate,  $n$ , is the outcome of an arbitrage between the carbon price  $p_C$ <sup>19</sup> and the backstop technology

(footnote continued)

time scales, induced by the change of radiative forcing resulting from a linear doubling of the atmospheric CO<sub>2</sub>-e concentration (at a 1% increase rate of the stock per annum, hence a doubling in about 70 years). The TCR denotes the deviation obtained at the end of this doubling, while the ECS accounts for the new equilibrium of the system, reached decades later due to its thermal inertia. In our setting, assuming the calibration given in Appendix E, we find a TCR of approximately 1.5, which is in line with IPCC (2013).

<sup>18</sup> As previously mentioned, the energy intensity,  $\sigma$ , passively declines, slowly improving the environmental performance of the economy.

<sup>19</sup>  $p_C$  refers to the price per ton of CO<sub>2</sub>-e.

**Table 1**  
Balance sheet, transactions, and flow of funds in the economy.

	Households	Productive sector	Banks	Sum
Balance sheet				
Capital stock		$pK$		$pK$
Deposits	$M^h$	$M^c$	$-M$	
Loans		$-L_c$	$L_c$	
Equities	$E$	$-E^f$	$-E^b$	
Sum (net worth)	$X^h$	$X^f = 0$	$X^b = 0$	$X$
Transactions		Current	Capital	
Consumption	$-pC$	$pC$		
Investment		$pI$	$-pI$	
Acc. memo [GDP]		$[pY]$		
Wages	$W$	$-W$		
Capital depr.		$(\delta + D^K)pK$		
Carbon taxes	$pT_f$	$-pT_f$		
Int. on loans		$-r_c L_c$	$r_c L_c$	
Bank dividends	$\Pi_b$		$-\Pi_b$	
Productive sector dividends	$\Pi_d$	$-\Pi_d$		
Int. on deposits	$r_M M^h$	$r_M M^c$	$-r_M M$	
Column sum (balance)	$S^h$	$\Pi_r$	$S^b$	
Flow of funds				
Change in capital stock		$p\dot{K}$		$p\dot{K}$
Change in deposits	$\dot{M}^h$	$\dot{M}^c$	$-\dot{M}$	
Change in loans		$-\dot{L}_c$	$\dot{L}_c$	
Column sum (savings)	$S^h$	$\Pi_r$	$S^b$	
Change in equities	$\dot{E}^f$	$-(\Pi_r + \dot{p}K)$		
Change in bank equity	$\dot{E}^b$		$-\dot{S}^b$	
Change in net worth	$S^h + \dot{E}$	$0$	$0$	$\dot{p}K + p\dot{K}$

price,  $p_{BS}$ .<sup>20</sup>

$$n := \min \left\{ \left( \frac{p_C}{p_{BS}} \right)^{\frac{1}{\delta-1}}; 1 \right\}. \tag{31}$$

The backstop technology is available at a passively declining price:

$$\frac{\dot{p}_{BS}}{p_{BS}} := \delta_{p_{BS}} \leq 0. \tag{32}$$

As for the carbon price, this will be treated as an exogenous variable whose exponential trajectory drives our various scenarios:

$$\frac{\dot{p}_C}{p_C} := \delta_{p_C}(\cdot) \geq 0. \tag{33}$$

Section 6 provides a numerical prospective analysis of the impact of such carbon trajectories.

### 3.4. Stock-flow Consistency

Table 1 displays the stock-flow consistency of our model. It can be readily checked, in particular, that the accounting identity

<sup>20</sup> For the sake of clarity,  $n$  can be seen as the solution of a cost-minimization program between the abatement cost,  $AY$ , on the one hand, and the carbon tax,  $p_C E_{ind}$ , on the other hand.

“investment = saving” always holds. Indeed, the monetary counterpart of our economy can now be made explicit:  $M$  stands for total deposits and equals  $M^h$ , the deposits of households, plus  $M^c$ , the deposits of the productive sector. Since dividends of both financial and non-financial entities are redistributed to households, the latter own both types of equities, respectively  $E^f$  and  $E^b$ . Notice that, since the banks’ financial balance is always zero, their equity,  $E^b$ , can safely be assumed constant. Similarly, we assume that the market value of the productive sector’s equity is constant (e.g., because stock markets are closed in this model). Moreover, it follows from Eq. (8) and the accounting identity

$$pY = \Pi + W + rD + pT_f + \delta_D pK = pC + pI$$

that  $W + \Pi_d + rD + pT_f = \dot{D} + pC$ . Consequently,  $\dot{M}^h = \dot{D} = \dot{L} - \dot{M}^f$  is the change in corporate debt equals the change in households’ saving.

## 4. Long-run Analysis

In this section, we provide a brief analysis of our model, with a focus on the asymptotic stability of its steady states.<sup>21</sup>

### 4.1. Reduced-form After the Energy Shift

The model presented in Section 3 boils down to a 16-dimensional nonlinear dynamical system. The economic and climate modules are coupled through: (i) emissions defined in Eq. (15) and (ii) damages specified in Eqs. (27), (28), and (29). Once the energy shift is fully completed, there are no longer any additional emissions. As a consequence, once carbon neutrality is achieved, the mean atmospheric temperature deviation,  $T_{eq}$ , remains asymptotically constant, while abatement efforts vanish:  $A_{eq} = 0$ .<sup>22</sup> The only remaining exogenous term of the climate module,  $F_{exo}$ , follows a linear path until 2100 where it reaches a plateau. Its upper limit is thus reached at every long-run equilibrium. As a result, damages,  $D^Y$  and  $D^K$ , converge towards finite limits,  $D^Y_{eq}$  and  $D^K_{eq}$ . Therefore, an analysis of the macroeconomic module at its long-run equilibrium (if any) can be performed.

The macroeconomic module reduces to the following system of non-linear differential equations:

$$\begin{cases} \dot{\omega} & = \omega[\phi(\lambda) - i - \alpha] \\ \dot{\lambda} & = \lambda[g - \alpha - \beta(N)] \\ \dot{d} & = -d(g + i) + \kappa(\pi) + \Delta(\pi) - \pi - \frac{\nu\delta_D}{1 - D^Y} \\ \dot{N} & = \beta(N)N \end{cases} \tag{34}$$

with, as auxiliary variables, the profit share, the unitary cost of production, as well as the growth rates of the population, the consumption price, and of the real output:

$$\begin{aligned} \pi &= 1 - \omega - rd - \left( \frac{p_C \sigma + \delta_D \nu}{1 - D^Y} \right), \\ c &= \omega + rd + \Delta(\pi) + \frac{\nu\delta_D}{1 - D^Y}, \\ \beta(N) &= q \left( 1 - \frac{N}{P^N} \right), \\ i &= \eta_p (mc - 1), \\ g &:= \frac{\dot{Y}}{Y} = \frac{\kappa(\pi)(1 - D^Y)}{\nu} - \delta_D. \end{aligned}$$

<sup>21</sup> By steady state, we mean, as usual, a state of the economy where the variables driving the reduced form system—namely the wage share, the employment rate, the private debt ratio, and the global workforce—remain constant, while auxiliary variables—such as real growth or inflation—rise at a constant pace.

<sup>22</sup> Once the energy shift is achieved, the emission reduction rate equals one, whereas both the energy intensity and the price of the backstop technology are null. As a result, abatement efforts vanish, see Eq. (30).

**Table 2**  
The four scenarios.

Scenario	No feedback loop	Low damage	Low damage K	High damage K
Damage type	–	Nordhaus	Nordhaus	Weitzman
Damage on output	–	Yes	Yes	Yes
Damage on capital	–	–	Yes	Yes

#### 4.2. Long-term Equilibria With No Inflation

To make some progress in the analysis, we assume no inflation ( $i = 0$ ). This restriction will of course be relaxed for our numerical analysis in Section 5, performed with the full-blown calibrated model. The system Eq. (34) then admits a “Solovian” equilibrium, characterized by a balanced growth path, whose real growth rate is  $g = \alpha$ —as in a standard Solow or Ramsey growth model.<sup>23</sup> At this long-run steady state, the profit rate is given by

$$\pi_{eq} = \kappa^{-1} \left( \nu \frac{\alpha + \delta(\mathbf{D}^K_{eq})}{1 - \mathbf{D}^Y_{eq}} \right).$$

As a consequence, an increase of the mean atmospheric temperature deviation will lead to higher investments, namely to the level needed to keep the economy on the balanced growth path despite damages induced by global warming. This increase will translate into a rise in the steady-state value of profit share,  $\pi_{eq}$ , and of the debt-to-output ratio,  $d_{eq}$ . This first channel makes explicit the destabilizing impact of global warming. The balanced growth path is characterized by

$$\begin{cases} \omega_{eq} &= 1 - \pi_{eq} - rd_{eq} - \frac{\nu\delta(\mathbf{D}^K_{eq})}{1 - \mathbf{D}^Y_{eq}}, \\ \lambda_{eq} &= \phi^{-1}(\alpha), \\ d_{eq} &= \frac{\kappa(\pi_{eq}) + \Delta(\pi_{eq}) - \pi_{eq} - \frac{\nu\delta(\mathbf{D}^K_{eq})}{1 - \mathbf{D}^Y_{eq}}}{\alpha}, \\ N_{eq} &= P^N. \end{cases} \quad (35)$$

Furthermore, the combined effects of the rise of the profit rate and of the debt ratio will penalize the wage share, as they mechanically reduce the amount of remaining undistributed income. More precisely,  $\omega_{eq}$  can be rewritten as:

$$\omega_{eq} = 1 - \frac{\alpha - r}{\alpha} \pi_{eq} - r \frac{\nu \frac{\alpha}{1 - \mathbf{D}^Y_{eq}} + \Delta(\pi_{eq})}{\alpha}. \quad (36)$$

Since the profit share,  $\pi_{eq}$ , increases as damages become more severe, a sufficient condition for the wage share to be reduced in the long run by global warming is that the equilibrium growth rate,  $\alpha$ , be greater than the interest rate,  $r$ .<sup>24</sup> Finally, the long-run employment rate,  $\lambda_{eq}$ , is a monotonic function of the steady-state real growth rate—a direct consequence of the short-term Phillips curve, see Eq. (14).

Turning to the local asymptotic stability of this balanced growth path, the partial derivative of  $d$  with respect to  $\omega$  at equilibrium leads to

<sup>23</sup> In our set-up, the workforce growth parameter,  $\beta$ , is null at the equilibrium courtesy of the demographic transition.

<sup>24</sup> This might come as a surprise at first glance, since  $g > r$  has been popularized as being the hallmark of increasing inequality in favor of capital. First, Giraud and Grasselli (2017) show that this alleged symptom is actually misleading. Second, here,  $r$  is the short-run interest rate, and is not necessarily equal to the return on capital. Last, along the transitional dynamics and absent damages,  $\omega = 1 - \pi - rd$ , so that Eq. (36) captures but the relationship between  $\omega$  and  $\pi$  at the Solovian steady state. Of course, this relationship will have to be re-examined with an endogenous interest rate, set, for instance, by the central bank, as a function of inflation. We leave this for further research.

the following necessary and sufficient condition:

$$r \left[ \left( \frac{d_{eq}}{\nu} (1 - \mathbf{D}^Y_{eq}) - 1 \right) \kappa'(\pi_{eq}) + (1 - \Delta'(\pi_{eq})) \right] < 0. \quad (37)$$

Details of its computation are given in Appendix A. A little algebra shows that, whenever  $r > 0$  and  $\omega$  decreases, local asymptotic stability of the balanced growth path requires  $d$  to increase, and vice-versa. This is broadly in line with what has been observed in the last decades in Western countries. As we shall see, the transitional dynamics with climate change and inflation might not necessarily lead to the Solovian steady state just described.

### 5. Prospective Analysis

We now turn to a numerical analysis of the impact of climate change along the transition path of the economy towards one of its steady states. By contrast with the previous section, this time we take due account of inflation. Let us first explore our four main scenarios, chosen for their illustrative qualities.

#### 5.1. The Four Main Scenarios

We calibrated our macroeconomic module at the world level using data from the World Bank, Penn University, the U.S. Bureau of Economic Analysis, and the United Nations,<sup>25</sup> while the climate module was calibrated on the Nordhaus DICE 2016R model through a method of moments. Appendix E reports the details of this calibration, and Appendix D provides the initial values of our integrated dynamics. The path of the world economy is simulated over the period 2016–2300 for the study of steady states—in order to account for the long-term inertial effects of climate on the economy—but we shall focus our inquiry of the transitional dynamics over the range 2016–2100 in line with the temporal horizon of climate policy-makers.

We consider four classes of scenarios, wrapped up in Table 2.<sup>26</sup> First, the *No feedback loop scenario* is a business-as-usual trajectory without climate feedback loop. This thought experiment will provide a macroeconomic benchmark, absent climate damages considerations. Second, the *Low damage scenario* introduces Nordhaus-type climate damages—where the functional form of the damage function is that of Nordhaus (2007), and damages are allocated only to the flow of production. It allows for a qualitative comparative analysis with the DICE model.<sup>27</sup> Third, and in line with the recent literature (Dietz and Stern, 2015; Lenton et al., 2008), the *Low damage K scenario* refines the impact of climate change, using the same damage function as Low damage scenario, but allocated to both output and capital. Fourth, the *High damage K scenario* takes advantage of Weitzman (2012) by introducing an alternative and more convex functional form of climate damages.

#### 5.2. The No Damage Case

Fig. 1 below presents the trajectory obtained in the No damage case and Table 3, some of its key figures. The (exogenous) deterministic

<sup>25</sup> More precisely, the behavioral aggregate functions (i.e., the Phillips curve, investment, and dividends) were calibrated, while the remaining parameters were calibrated. More details on our calibration are available in Appendix E and our method in Appendix C. Further details about our methodology are available upon request.

<sup>26</sup> Of course, a number of other scenarios are conceivable—e.g., by coupling an endogenous temperature-driven productivity with a given damage function, etc. They are available upon request.

<sup>27</sup> Both models differ in their macroeconomic cores and initial values but share identical climate module, climate feedback loop, and allocation of damages. Otherwise stated, DICE and our model under the *Low damage scenario* differ only through their macro-dynamics. The next scenarios introduce damages specifications that differ from DICE.

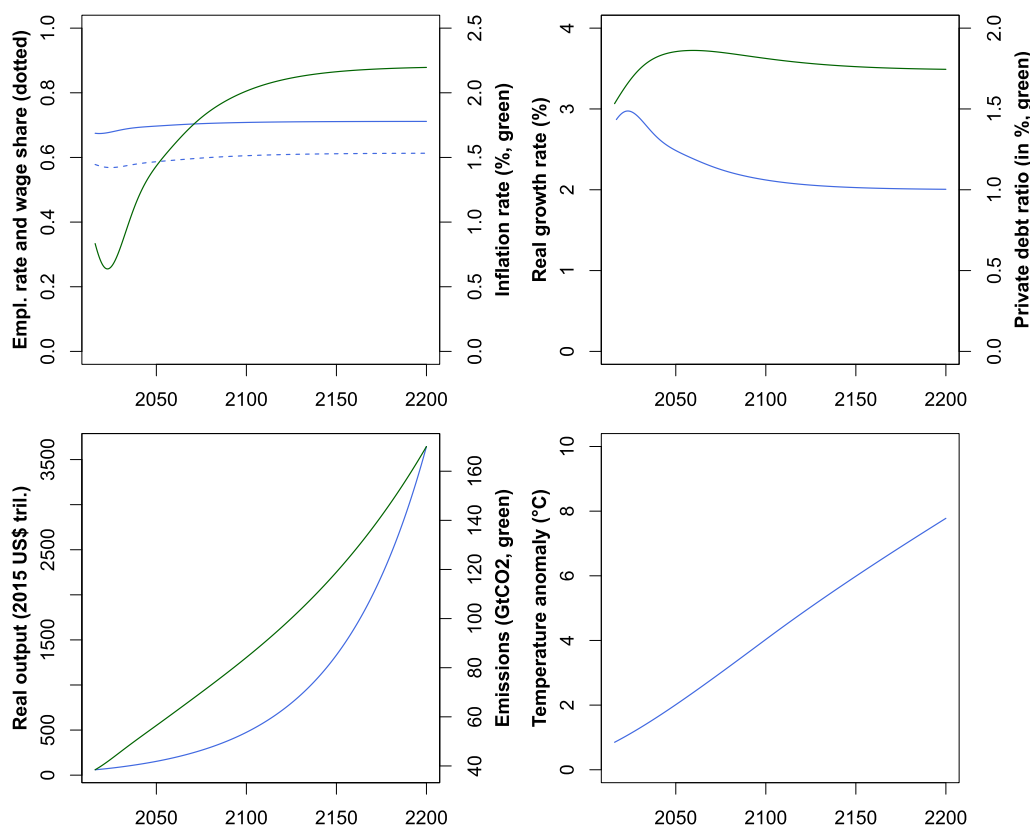


Fig. 1. Trajectories of the main simulation variables in the *No feedback loop scenario*.

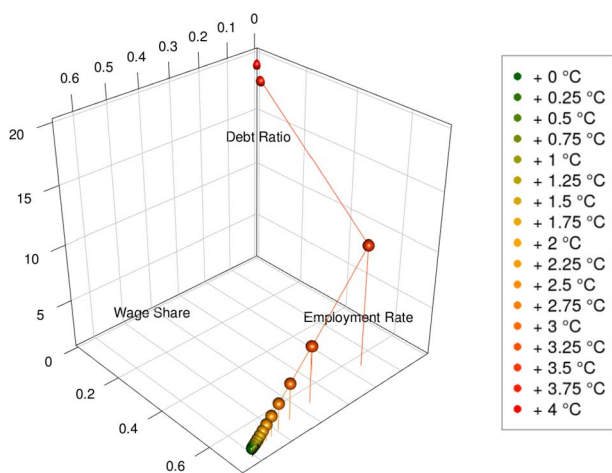


Fig. 2. Solovian steady state as a function of temperature anomaly in the *High damage K scenario*.

exponential growth of productivity,  $a$ , feeds the rise of real GDP, which in 2100 reaches eight times its initial 2015 volume.<sup>28</sup> Here, inflation starts at approximately 0.5%, and converges in the range of 2–2.5% *per annum*. The employment rate stabilizes around 70%—close to the current world average value. The wage share converges in the vicinity of 60%, and the debt-to-output ratio stabilizes around 180% (slightly above its current level). In other words, absent any climate feedback loop, the world economy converges towards a balanced growth path.

<sup>28</sup> At variance with Goodwin (1967), the trajectories obtained in Fig. 1 display few oscillations. This is the consequence both of the introduction of private debt (which turns the conservative dynamical system into a dissipative one) and inflation. This confirms a remark already made by Grasselli and Nguyen-Huu (2015a): inflation has a dampening effect on the endogenous real business cycles of the underlying Lotka-Volterra dynamics.

However, it is worth mentioning that our calibration is compatible with the economy converging to the “bad” attractor once global warming is taken into account. What Fig. 1 actually shows is therefore that our world economy belongs to the basin of attraction of the desirable long-run equilibrium. Notice, nevertheless, that Fig. 1 exhibits a sharp increase of CO<sub>2</sub>-e emission, resulting in an increase of the temperature anomaly of approximately +10°C. As we shall see, the climate feedback loop will have a destabilizing effect.

Indeed, we saw in Section 4 that climate damages tend to reduce the wage share. Since, for simplicity, in this paper inflation is cost-push, global warming might thus lower inflation and consequently increases the debt-to-GDP ratio. Can these effects distract the world economy from converging towards the balanced growth path?

### 5.3. Long-term Analysis

To address this question, and echoing the discussion of Section 4, let us first consider how the long-run Solovian equilibrium is numerically affected by global warming in the phase diagram  $(\omega, \lambda, d)$ . In this subsection, we therefore treat the temperature anomaly as an exogenous parameter (independent of abatement costs and emissions) and plot the corresponding long-run balanced growth path. To do so, we used the world calibration detailed in Appendices D and E, to simulate the system Eq. (34) together with an exogenously given temperature deviation (and its associated damages). We then numerically identified the long-run equilibrium. In the following subsection, we provide a geometric view of the destabilizing effect of global warming through its influence on the basin of attraction of the long-term steady state.

#### 5.3.1. Solovian Steady and Temperature

For the sake of illustration, we only illustrate the *High damage K scenario*. The other scenarios exhibit a similar relationship between debt and temperature anomaly, with a bifurcation occurring at a higher temperature anomaly (the damage function is less convex). The

corresponding results are available upon request. As shown by Fig. 2, when temperature rises, the economy first keeps following the balanced growth path and therefore converges towards a Solovian equilibrium. Between +3 °C and +4 °C, however, a bifurcation occurs, after which the world economy ends up in a deep economic recession in which damages induced by global warming can no longer be offset. The corresponding long-run attractor exhibits zero wage share and employment rate together with an unbounded debt ratio.

This echoes Lenton et al. (2008), who conclude using completely different methods that the +4 °C threshold may indeed be a tipping point for the climate system. Our simulations further suggest that, prior to this tipping point, the long-run employment rate should be close to 70%, the equilibrium wage share should shrink to 50%, and private debt should equal approximately ten times the world's GDP.

### 5.3.2. A Geometric View of the Destabilizing Effect of Global Warming

Climate change impacts the macro-dynamics of the world economy inasmuch as it makes the Solovian long-run equilibrium more difficult to reach. A bifurcation occurs whenever the “climate perturbation” is strong enough to prevent the economy from converging towards this desirable steady state. In terms of public policies, the trouble with this conclusion is: 1) that the modifications induced by climate change on the Solovian equilibrium highlighted in Fig. 2 are a long-term phenomenon that may not be noticeable in the short run—it might be that our world economy is already following a path towards a bad attractor without exhibiting much difference, in the short-term, from trajectories that would lead to a balanced growth path. Then 2), the rise in temperature is treated as an exogenous variable whereas it in fact depends upon the actual path followed by the economy. This prompts two questions: can we infer the long-run dynamics of our economy from short-run information?

We address these questions from a geometric perspective by comparing the basins of attraction of the desirable steady state with and without climate change. From this subsection on, the linkage between economic and climate dynamics are considered. Varying initial conditions will possibly lead to various emission paths, hence to different equilibrium temperature deviations and eventually to different “desirable” equilibria (whenever the latter are still attainable). Given some specified emission-reduction rate path, we shall consider the set of *all* initial conditions that do *not* lead to an economic cave-in. Let us call this set the “good” basin of attraction.

In order to numerically approximate the “good” basin of attraction, we started with a reasonable range of initial conditions for the variables of interest (wage share, employment rate, debt ratio), outside of which the world economy is definitely not viable.<sup>29</sup> We then considered another compact set to which long-term solutions had to belong in order to be considered as economically desirable (hereafter the “convergence set”).<sup>30</sup> Any long-run steady state outside of this convergence set could not justifiably be claimed to be a “good” equilibrium. Finally, we assumed a common emission-reduction rate path for the world economy defined here as the minimal path avoiding a collapse, given the postulated initial conditions.<sup>31</sup> We then computed the trajectory starting anywhere in the initial set and checked whether it ended up in the convergence set at a large time scale. Whenever this was the case, the starting point was then

<sup>29</sup> Our initial set is:  $(\omega, \lambda, d) \in [0.2 : 0.99]^2 \times [0.1 : 2.7]$ . The choice of 2.7—the constant capital-to-output ratio—is a threshold value so that if  $d > 2.7$ , we have  $D > pK$ . In other words, the level of nominal debt is higher than the market value of capital. Such a situation will most likely lead to a substantial amount of bankruptcy not modeled in this paper, since existing capital is the only available collateral for debt, see Fostel and Geanakoplos (2015).

<sup>30</sup> The convergence set is:  $(\omega, \lambda, d) \in [0.4 : 0.99]^2 \times [0.1 : 2.7]$ .

<sup>31</sup> More precisely, we considered an initial real carbon price of 2010 US\$ 2 t/CO<sub>2</sub>-e<sub>2</sub> in 2016, in line with the exogenous backstop technology path, and its associated minimal constant growth rate necessary to avoid a recession (under the initial conditions presented in Appendix D).

considered to be part of the “good” basin of attraction.

We carried out this thought experiment assuming alternatively (i) no climate feedback loop or (ii) environmental damages of the *Low damage scenario*. Fig. 3 plots the “good” basin of attraction obtained in the former case. It turns out that almost all (reasonable) initial conditions lead to the convergence set. This emphasizes the robustness of the calibration of the *No feedback loop scenario*: absent climate change, the world economy converges to some rather desirable long-run steady state almost independently of its starting point. By contrast, the right side of Fig. 3 displays the “good” basin of attraction obtained in the latter case.<sup>32</sup>

Global warming obviously narrows the set of initial conditions that allow our world economy to avoid an economic recession. Interestingly enough, the higher the wage share today and the higher the employment rate, the easier it will be for the world economy to circumvent a disaster. This is not surprising given the positive impact of climate damages on the profit share: the need to invest more so as to compensate for losses in output and capital will favor the distribution of wealth towards capital holders. One way to compensate for this trend is to have an initial distribution biased in favor of labor. Since  $\pi$  is only a ratio, this, of course, does not imply that investors will be better off with climate change than without. Nonetheless, to the best of our knowledge, Fig. 3 provides the first analytical link between climate change and the classical capital-labor distribution of wealth issue: a more resilient economy is, in our setting, one where labor is favored. Notice as well that resilience against global warming also calls for less private debt: an initially over-indebted economy turns out to be incapable of carrying the burden of new debt resulting from additional investment triggered by climate damages.

### 5.4. Transitional Dynamics

We finally present our prospective trajectories. For each scenario presented in Subsection 5.1, we first examine the trajectory obtained together with a rather mild emission-reduction rate path, close to the one considered by Nordhaus and Sztorc (2013). This policy is based on a real carbon price fixed in 2016 at an initial value of 2010 US\$ 2 t/CO<sub>2</sub>-e<sub>2</sub>.<sup>33</sup>

The results can be observed in Fig. 4, while Table 3 provides other key indicators regarding those four scenarios.

As expected, global warming systematically penalizes output: the compound annual real growth rate (CAGR), in Table 3, between 2010 and 2100, remains systematically below the 2.50% level of the *No feedback loop scenario*. Besides, the temperature deviation in 2100 is systematically above +3 °C. Moreover, climate change increases potential financial instability by pushing up the private debt ratio, above the 181% level of the *No feedback loop scenario*.

A distinction emerges depending upon whether damages affect output only (*Low damage scenario*) or are allocated between output and capital (*Low damage K scenario* and *High damage K scenario*). Indeed, whenever climate disturbance inflicts direct damages on capital, the latter permanently reduces potential output (Dietz and Stern, 2015). As a result, the world productive sector is forced to leverage in order to finance investment, which fuels a rise of the debt-to-GDP ratio (202% in the *Low damage scenario* and 335% in the *High damage K scenario* in 2100). Moreover, real output is penalized, ultimately generating disruptive effects on the labor market. In the *High damage K scenario*, the resulting financial turmoil drives the economy towards a global

<sup>32</sup> The computation of the “good” basins of attraction for other types of damage and allocation leads to similar results, namely, that as damages become more severe, the set of acceptable initial conditions under which a collapse may be avoided shrinks dramatically.

<sup>33</sup> This value is chosen so as to be compatible with an initial emission reduction rate of 3% and the initial condition for the price of the backstop technology. Again, the details of the calibration are given in Appendix E and D, together with an average growth rate of 2% per year.

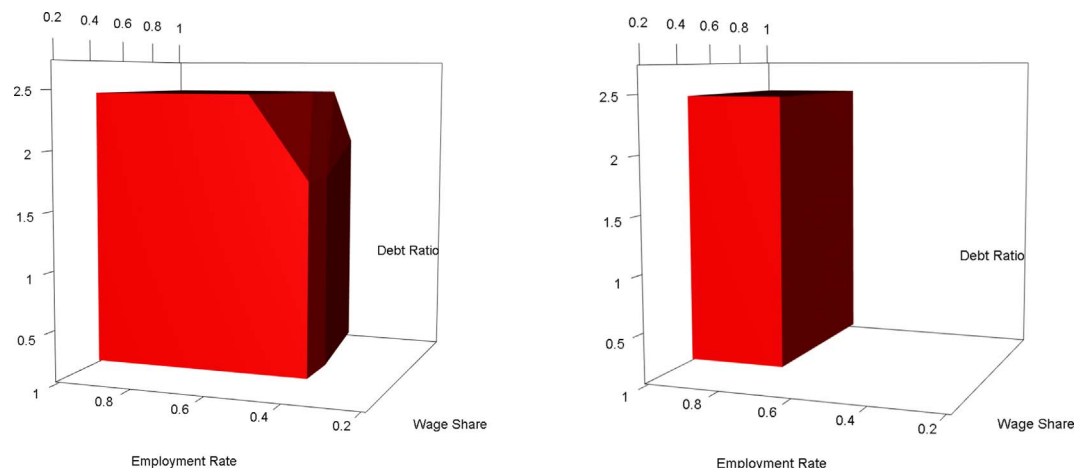


Fig. 3. “Good” basins of attraction in the *No feedback loop scenario* (left) and in the *Low damage scenario* (right).

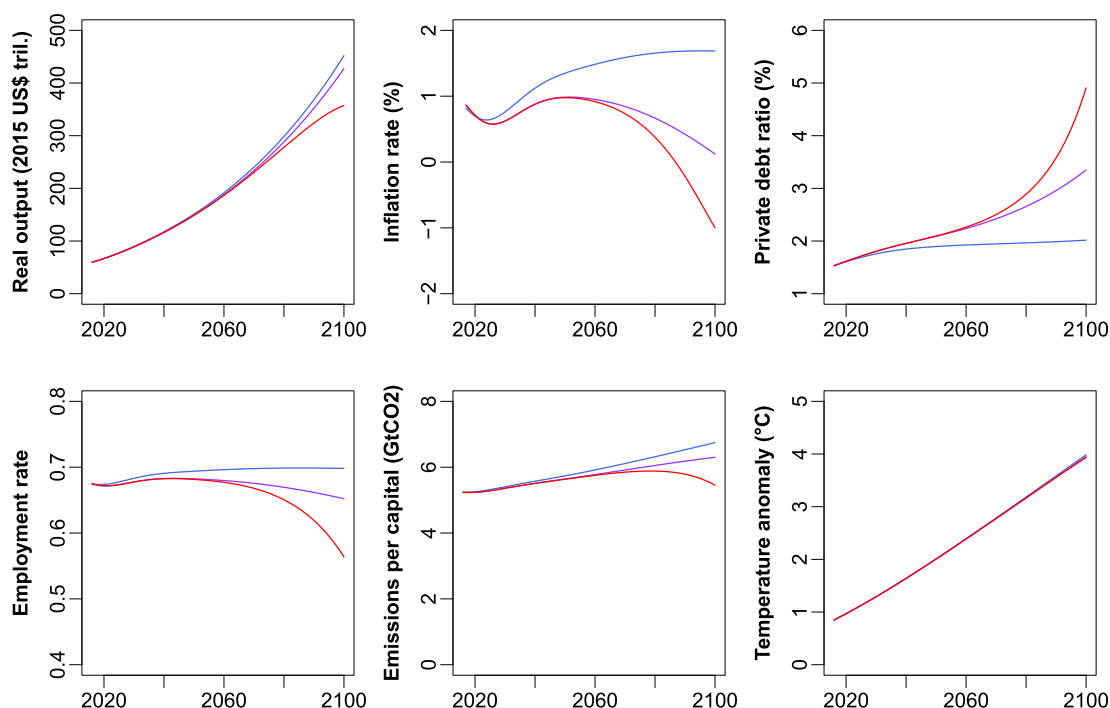


Fig. 4. Macroeconomic trajectories without proactive public policies in the *Low damage scenario* (blue line), *Low damage K scenario* (purple line) and *High damage K scenario* (red line). (For interpretation of the references to color in this figure legend, the reader is referred to the web version of this article.)

Table 3  
Key values of the world economy.

Scenario	No feedback loop	Low damage	Low damage K	High damage K
CAGR of real GDP w.r.t. 2010–2100	2.50%	2.44%	2.37%	2.15%
Private debt ratio in 2100	1.81	2.02	3.35	4.91
CO <sub>2</sub> -e emissions per capita in 2050	–	5.74 t CO <sub>2</sub> -e	5.65 t CO <sub>2</sub> -e	5.64 t CO <sub>2</sub> -e
Temperature change in 2100	–	+3.99 °C	+3.95 °C	+3.94 °C
CO <sub>2</sub> -e concentration in 2100	–	819 ppm	804 ppm	792 ppm

recession in the next century if no voluntary public policy is implemented. This is illustrated by the phase diagram in the  $(\omega, \lambda, d)$  space of Fig. 5 below where the employment rate indeed falls to zero while

the debt ratio explodes.<sup>34</sup>

*Low damage K* and *High damage K* scenarios thus illustrate that degrowth (by disaster, not by design) might already start at the turn of the next century in the *High damage K* case. This shows that, within the conditions embodied in our last two scenarios, and unless appropriate public policies are implemented, today's world economy lies outside the basin of attraction of the Solovian equilibrium. Finally, it is worth mentioning that the type of degrowth just alluded to is characteristic of Fisherian debt-deflation (Fisher, 1933), as negative inflation rates prevail while private debt skyrockets, as observed in Fig. 4.

We now turn to proactive emission-reduction paths implemented through a carbon price instrument so as to bring the world economy as close as possible to the +2 °C objective.

<sup>34</sup> Of course, introducing default would make it possible to get rid of the unrealistic feature of unbounded private debts. This task is left for future research.

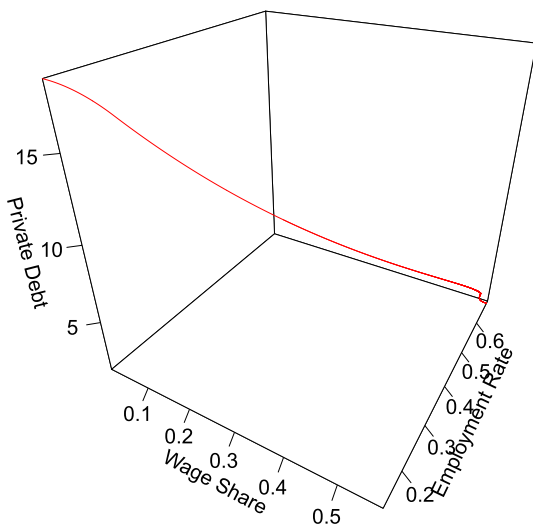


Fig. 5. Phase diagram for the *High damage K scenario* over the period 2016–2130. The initial condition is located in the bottom right of the figure.

6. Target Achievements

Given the exogenous backstop technology (borrowed from Nordhaus, 2016), the higher the trajectory of the carbon price, the faster the emission-reduction rate, as it becomes more costly to continue emitting greenhouse gases. In recent decades, two main targets have been discussed on the international scene: +1.5 °C and +2 °C.<sup>35</sup> In this section, we assess the reachability of such objectives through a carbon price. We first show that, absent carbon storage technologies, these objectives have become too ambitious. We then investigate the climatic, economic and financial sustainability of a continuum of trajectories characterized by a wide range of carbon prices. Lastly, we select two carbon price trajectories and analyze their transitional dynamics. Moreover, we contrast our results with other carbon price paths taken from Nordhaus (2016), the High-Level Commission on Carbon Prices (2017), and the IPCC (2013). To do so, we mainly focus on the *Low damage scenario* which is the closest to IAM's benchmarks.

6.1. Which Targets can be Reached?

Our conclusion on the +2 °C target is clear, and amply confirms the one reached by Nordhaus (2016), though using an entirely different economic model: without capture and storage of carbon, it will be almost impossible to achieve this goal unless, climate sensitivity turns out to be equal to its low values (below 3 °C). This is illustrated by Fig. 6, which yields the value of climate sensitivity (introduced in Subsection 3.2 *supra*) versus the temperature anomaly whenever carbon neutrality has been achieved in 2016.<sup>36</sup> As expected, the higher the climate sensitivity, the higher the temperature anomaly reached in 2100. For a climate sensitivity of 3.1,<sup>37</sup> the temperature anomaly in 2100 is +2.022 °C. We now examine the feasibility of less demanding temperature objectives under the assumption of a climate sensitivity (ECS) equal to 3.1.

<sup>35</sup> Both targets are mentioned by the Paris Agreement (Art. 2).  
<sup>36</sup> For the sake of precision, (i) the heat capacity of the atmosphere *C* is updated according to the climate sensitivity in order to account for the changes in the TGR when the ECS changes as in Nordhaus and Sztorc (2013), (ii) carbon storage is precluded, and (iii) land-use related emissions, that are not directly related to industrial activities and marginally affect the temperature dynamics, are maintained.  
<sup>37</sup> 3.1 is approximately the mean value of the distribution log -  $\mathcal{N}(\mu = 1.10704, \sigma = 0.264)$  reported in Gillingham et al. (2015).

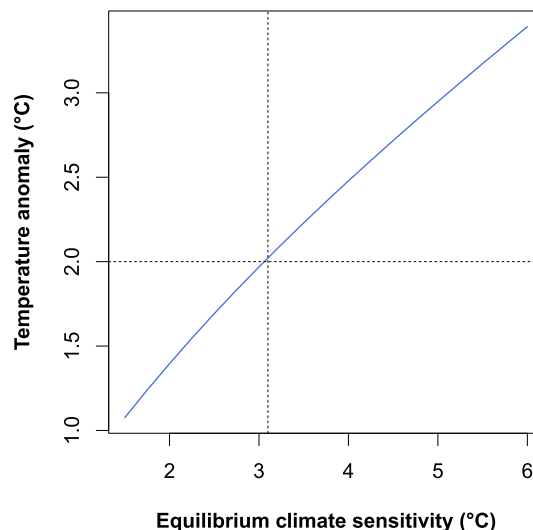


Fig. 6. Temperature increase in 2100 as a function of climate sensitivity whenever zero net emission is reached in 2016.

6.2. Climate, Economic and Financial Trade-offs

Let us now turn to the sustainability of plausible climate and economic trajectories. We chose to use an exogenous carbon price because of the well-known difficulty in eliciting the “right” discount rate (Sterner and Persson, 2008). A simple parametric carbon price function will therefore be considered:

$$\frac{\dot{p}_C}{p_C} = a_{p_C} + \frac{b_{p_C}}{t} \tag{38}$$

where  $a_{p_C} \geq 0$  stands for a long-term growth rate trend of the carbon price and  $b_{p_C}/t \geq 0$  represents the time-varying component of the growth rate, with *t* the number of years since the policy is active (i.e.  $t_{2016} = 1$  in 2016, the starting point of our simulations). This formalization allows for an initial ramp-up period of the carbon price growth, followed by the convergence over time towards a constant, asymptotic trend  $a_{p_C}$ . This carbon price implementation profile is compatible with seminal contributions such as IPCC (2013) or the High-Level Commission on Carbon Prices (2017)—as illustrated in the bottom left panel of Fig. 9. For now, Fig. 7 provides some representative patterns of the parametric function going from fast energy shifts as advocated, for example, by Nicholas Stern—with a carbon pricing initially more convex than in the exponential case—to slower transitions, closer in spirit to William Nordhaus' contributions.<sup>38</sup>

The heatmaps in Fig. 8, based on the two parameters of the carbon price trajectory in Eq. (38), encapsulate the climate, economic and financial consequences of a wide variety of carbon prices. For that purpose, we selected three indicators: (i) the temperature anomaly in 2100; (ii) the minimum of the real growth rate throughout the century; and (iii) the maximum debt-to-GDP ratio throughout, as a proxy for financial stability.<sup>39</sup> For instance, the temperature anomaly goes from +2 °C in green to +4 °C in dark red. The resulting heatmaps are plotted in Fig. 8 for the temperature anomaly and the minimum of the real growth rate. The heatmap of the maximum debt-to-GDP ratio, given in Appendix B, mimics the one obtained for the temperature anomaly: a lower temperature increase in 2100 is accompanied with a lower level

<sup>38</sup> Either way, whenever the carbon price hits the price of the backstop technology, zero net emission prevails — the carbon price then decreases exponentially, at the pace of the back-stop technology.

<sup>39</sup> Those three indicators are computed for a total of 1600 combinations of  $(a_{p_C}, b_{p_C})$  within the set  $[0; 0.2] \times [0, 1]$ . For each combination, the model is simulated and the value found for each indicator is reported with a specific color.

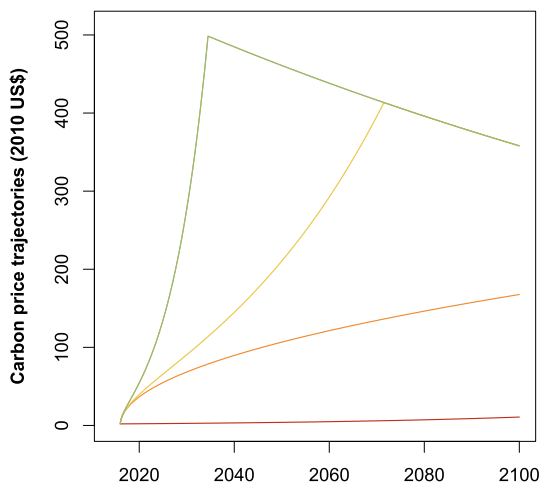


Fig. 7. Examples of carbon price paths generated from Eq. (38).  $(a_{p_C}, b_{p_C}) = (.02, 0)$  in red,  $(a_{p_C}, b_{p_C}) = (0, .5)$  in orange,  $(a_{p_C}, b_{p_C}) = (.02, .5)$  in yellow and  $(a_{p_C}, b_{p_C}) = (.1, .5)$  in green. (For interpretation of the references to color in this figure legend, the reader is referred to the web version of this article.)

of debt-to-output ratio, as already discussed. The left-hand side of Fig. 8 shows that, with very high carbon prices in the short term, the temperature anomaly can be limited to  $+2.07^\circ\text{C}$ . However, the right-hand side of Fig. 8 suggests that such victory on the climate front would be achieved at the cost of a deep worldwide economic recession: the real “growth” rate in 2100 would be close to  $-5\%$ . As for the private debt ratio, it roughly follows the temperature anomaly, and not real growth. This should not come as a surprise, as already discussed in Section 4.

These findings shed new light on the current trade-offs faced worldwide by public policy. In order to avoid possible severe climate-induced financial and economic injuries, the optimal region lies in the blue area of the right hand side of Fig. 8 and as close as possible to the dark green on the left hand side. With, for example,  $(a_{p_C}, b_{p_C}) = (0.125, 0.625)$ , real degrowth rate would presumably be avoided throughout the century, and the rise of Earth’s temperature would be probably capped below  $+2.5^\circ\text{C}$ .

Building on these insights, we finally analyze what seems to be more realistically achievable goals—namely a  $+2.5^\circ\text{C}$  and  $+3^\circ\text{C}$  limitation of global warming—achieved with economically sustainable carbon price paths.

### 6.3. Policy Goals: $+2.5^\circ\text{C}$ and $+3^\circ\text{C}$ in 2100

To simplify the discussion, we selected two trajectories within the continuum of possibilities illustrated by Fig. 8 that are found compatible with a  $+2.5^\circ\text{C}$  and  $+3^\circ\text{C}$  target respectively. To do so, we set the maximal value of the short-term ramp-up,  $b_{p_C} = 0.5$ , which avoids any decrease in GDP throughout the century. Then, we chose maximal  $a_{p_C}$  that meets the given temperature targets. Fig. 9 plots the results in the *Low damage scenario*. In this setting, a carbon price of, for example., approx 2010 US\$2 in 2016, \$44 in 2020, \$140 in 2030, and \$300 in 2040 per GtCO<sub>2</sub>-e would be required to achieve a  $+2.5^\circ\text{C}$  objective in 2100. For a  $+3^\circ\text{C}$  goal, the figures would be approx. 2010 US\$2 in 2016, \$38 in 2020, \$83 in 2030, and \$125 in 2040, \$172 in 2050 and \$224 in 2060 per GtCO<sub>2</sub>-e.

Trajectories in green (resp. in cyan) exhibit a mean atmospheric temperature of  $+2.5^\circ\text{C}$  (resp.  $+3^\circ\text{C}$ ) at the end of this century, courtesy of an energy shift achieved around 2045 (resp. 2080). This means that carbon neutrality needs to be reached at the world level as early as 2045 (resp. 2080) if the  $+2.5^\circ\text{C}$  (resp.  $+3^\circ\text{C}$ ) is to be met.<sup>40</sup> Other scenarios than the *Low damage scenario* show almost identical

patterns—with the exception of the debt-to-output ratio, which is displayed in dashed curves for the *High damage K scenario*.

For the sake of compatibility with previous findings on carbon prices, we plot in Fig. 9 the outcomes of our model, in various shade of grey, for carbon prices taken from *High-Level Commission on Carbon Prices (2017)*, *IPCC (2013)*, *Nordhaus (2016)*.<sup>41</sup> We note that the three lower paths (IPCC Low, Stern-Stiglitz Low, and Nordhaus) show a temperature increase in 2100 almost at  $+3.5^\circ\text{C}$ , while Stern-Stiglitz High meets the  $+3^\circ\text{C}$  and the IPCC High is somewhere between  $+2.5$ – $3^\circ\text{C}$ .

Comparing the  $+2.5^\circ\text{C}$ , in green, trajectories with their  $+3^\circ\text{C}$  counterparts, in cyan, the main difference is that the real GDP in 2100 is 1% higher as the temperature is lower. This means that, by the end of the century, the extra abatement cost of reducing the temperature anomaly by  $+0.5^\circ\text{C}$  will pay off as it makes damages less harmful to the economy, which is consistent with the findings of Fig. 8. Moreover, Fig. 9 shows that the real output drops whenever the emission-reduction effort is put into practice. This phenomenon is amplified as the transition date intervenes earlier.

When analyzing the different shapes of carbon price, especially in the short run, the employment rate shows the potential short run recessionary followed by an economic recovery of a sudden increase of the carbon price. Indeed, comparing the  $+3^\circ\text{C}$  trajectory to Stern-Stiglitz High illustrates this point as they both meet the same target of  $+3^\circ\text{C}$ . Stern-Stiglitz High shows an early increase pattern followed by a rather small and steady growth rate, while the  $+3^\circ\text{C}$  trajectory starts rather low and finishes high. As a consequence, the short term employment rate is lower for the Stern-Stiglitz High than its counterpart. However, from 2035 on, this relation is inversed and the employment rate is greater in the Stern-Stiglitz High simulation.

Turning to the private nonfinancial corporate debt ratio, the effect of the abatement cost can also be seen on the debt-to-output ratio: in 2050 (resp. 2100) the  $+2.5^\circ\text{C}$  (resp.  $+3^\circ\text{C}$ ) trajectory exhibits a debt-to-output ratio of 2.27 (resp. 2.22) while its  $+3^\circ\text{C}$  counterpart is 1.93 (resp. 2.2). A faster energy-shift clearly translates into a greater potential source of financial instability.<sup>42</sup>

Last, when running these simulations within a more realistic setup—the *High damage K scenario*—, where environmental damages are also factored into the depreciation rate of capital, we see that the world economy is facing a run-up of debt. In 2100, our simulations show a 3.1 (resp. 3.57) debt-to-GDP ratio for the  $+2.5^\circ\text{C}$  trajectory (resp.  $+3^\circ\text{C}$ ). These values raise a red flag: whenever nominal debt becomes higher than money capital (which usually serves as collateral), a cascade of defaults is to be expected, along the storyline analyzed (in a static framework) by *Fostel and Geanakoplos (2015)*.

## 7. Conclusion

By combining financial and environmental features, the stock-flow consistent macroeconomic model introduced in this paper allows us to examine the conditions for economic growth depending on the damages induced by global warming and a carbon price path. To our knowledge, this is the first dynamic model calibrated at the world level that enables both environmental and financial risks to be assessed within a framework of endogenous monetary business cycles.

Our main findings are as follows. First, the  $+2^\circ\text{C}$  target seems to be already out of reach unless climate sensitivity luckily turns out to be low (below  $3^\circ\text{C}$ ) or if negative emission technologies were developed at the world scale in the coming decades. Second, our simulations shed new light on the interplay between economic (GDP growth and

<sup>41</sup> That are the 25<sup>th</sup> and 75<sup>th</sup> percentile reported in the middle range of Figure TS.12 in *IPCC (2013)*, the optimal trajectory in *Nordhaus (2016)*, and the 2020–30 values reported in *High-Level Commission on Carbon Prices (2017)* assumed to be in 2005US\$.

<sup>42</sup> This confirms the warning strongly expressed by Governor Mark Carney in September 2015 *Carney (2015)*.

<sup>40</sup> This is in line, e.g., with the *Deep Decarbonization Pathways Project (2015)*.

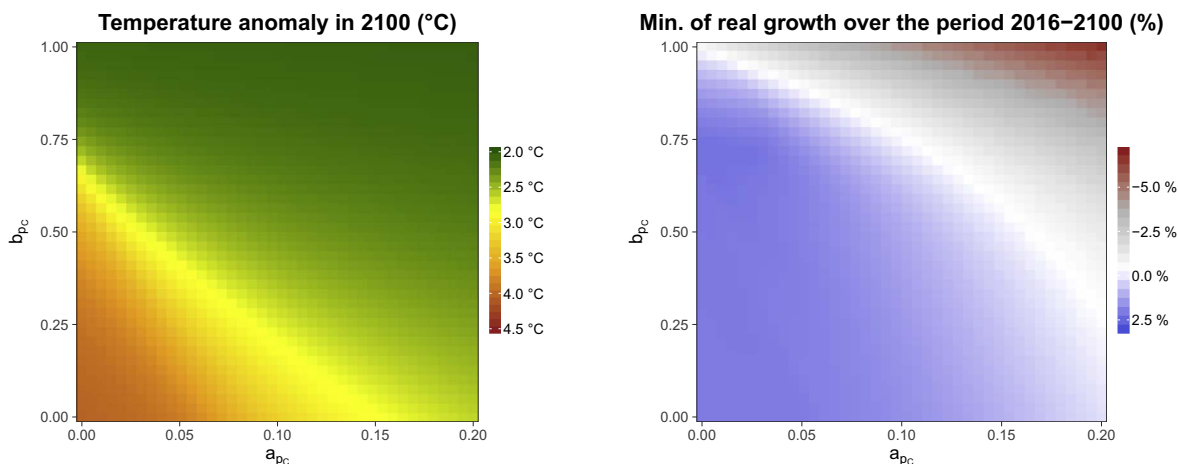


Fig. 8. Heatmaps of the temperature anomaly in 2100 (left side) and minimum of the real output growth rate over the period 2016–2100 (right side) in the *Low damage K scenario* with ECS = 3.1. (For interpretation of the references to color in this figure, the reader is referred to the web version of this article.)

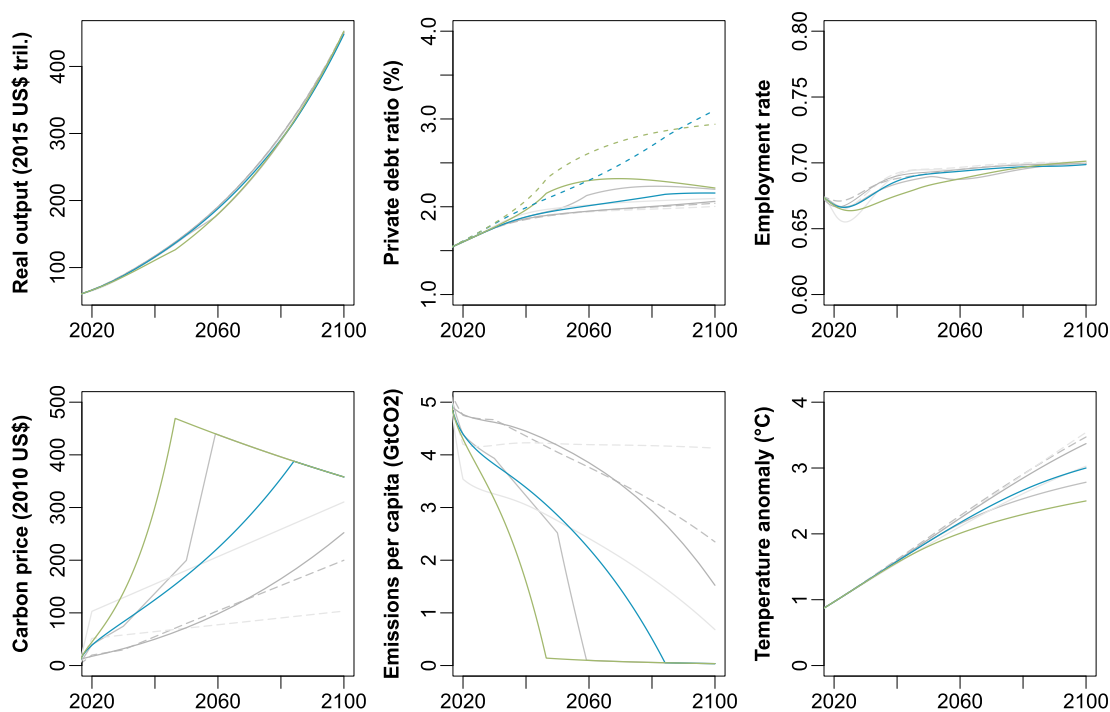


Fig. 9. Trajectories of the main variables in the *Low damage scenario*. The represented carbon price trajectories corresponds to: (i) the IPCC Low case (dashed grey), (ii) the IPCC High case (solid grey), (iii) the Stern-Stiglitz Low case (light dashed grey), (iv) the Stern-Stiglitz High case (light grey), (v) the Nordhaus case (dark grey), (vi) the model 2.5 °C case (green curves), and the model 3 °C case (cyan curves). Additional trajectories in the *Low damage K scenario* are given in dashed colored curves. (For interpretation of the references to color in this figure legend, the reader is referred to the web version of this article.)

underemployment), financial (level of private debt) and climate instabilities. Indeed, they reinforce each other and may ultimately lead to an unintended planet-wide economic degrowth at the end of this century (cf. our *High damage K scenario*). However, our results suggest that, together with a “right” carbon price path, redistributing wealth in favor of wages, fostering employment, and reducing the private debt-to-output ratio, would make it easier for today’s world economy to find a growth path that will ultimately circumvent a recession despite injuries induced by a hotter planet. Third, the implementation of an adequate policy of emission-reduction through the deployment of a carbon price enables long-term prosperity to be restored, at least whenever climate sensitivity does not exceed 3.1°C. According to the simulations performed in this paper, however, the binding carbon price trajectory must be such that zero net emissions be reached as early as 2045 and, in any case, before 2080 in order to maintain global warming below +3 °C. For

instance, within the family of price functionals considered in this paper, the minimal carbon price trajectory compatible with the achievement of a +2.5 °C objective requires to setting of 2010 US\$44 in 2020, \$140 in 2030, and \$300 in 2040 per GtCO<sub>2</sub>-e.

At last, this paper calls for a number of extensions. Would a more elaborate public-policy scheme, incorporating both taxation and distribution tools, favor the resilience of the world economy to climate change? Would some (more realistic) degree of substitutability between capital and labor ease the compensations of climate damages borne by the private sector? Finally, throughout the paper, demographic trends have been taken as exogenous. How would its endogenization, both incorporating a climate feedback loop and the implementation of possible family policy, help to reach climate and economic sustainability? We see these questions as crucial challenges for further research along with the financial dimension of climate issues investigated in this paper.

**Acknowledgments**

The authors are grateful to three anonymous referees for their fruitful comments and suggestions. A special thank is due to Ekaterina Zatssepina for her technical assistance. We thank George Akerlof, Ivar Ekeland, Matheus Grasselli, Marc Lavoie, Hervé Le Treut, Antonin Pottier, Nicholas Stern, Joseph Stiglitz and participants of the World Bank Conference “The State of Economics. The State of the World” (June 16, 2016), of the OECD Development Centre Seminar, of the

Italian Association of Energy Economists’ Conference (Italy, December 2016), the Symposium for the Stern-Stiglitz High-level Commission on Carbon Pricing (Paris, March 2017), as well as the World Congress of the International Association of Economists (Mexico, June 2017) for their helpful advice. This work benefited from the support of the Chair Energy & Prosperity and the financial support of the *Agence Nationale de la Recherche* (project MeET-MaDyS; ref: ANR-15-CE05-0028). All remaining errors are our own.

**Appendix A. Stability of the Solovian Steady State**

Turning to the local asymptotic stability analysis of the long-run “good” equilibrium, the Jacobian matrix of the dynamic system reads

$$M(\omega_{eq}, \lambda_{eq}, d_{eq}, N_{eq}) = \begin{bmatrix} 0 & M_{12} & 0 & 0 \\ -M_{21} & 0 & -rM_{21} & M_{24} \\ M_{31} & 0 & M_{33} & 0 \\ 0 & 0 & 0 & M_{44} \end{bmatrix},$$

where the entries  $M_{ij}, (i,j) \in [[1;3]]$  are given by:

$$M_{12} := \omega_{eq} \phi'(\lambda_{eq}) > 0,$$

$$M_{21} := \frac{\lambda_{eq}}{\nu} \kappa' (p i_{eq}) (1 - D^Y_{eq}) > 0,$$

$$M_{24} := \lambda_{eq} \frac{q}{pN},$$

$$M_{31} := \frac{d_{eq}(1 - D^Y_{eq}) - \nu}{\nu} \kappa' (\pi_{eq}, D^Y_{eq}) - \Delta'(\pi_{eq}) + 1,$$

$$M_{33} := rM_{31} - \alpha,$$

$$M_{44} := -\frac{q}{pN}.$$

Then, the characteristic polynomial  $\chi_M(\cdot)$  of the Jacobian matrix at the “good” equilibrium writes

$$\chi_M(\epsilon) = \left( \epsilon + \frac{q}{pN} \right) [\epsilon^3 + (\alpha - rM_{31})\epsilon^2 + \dots + M_{12}M_{21}\epsilon + g_{Y_{eq}}M_{12}M_{21}].$$

The first root,  $\epsilon = -\frac{q}{pN}$ , of the polynomial  $\chi_M(\cdot)$  being obviously negative, the stability of the “good” equilibrium is given by the sign of the root of its factored polynomial of degree 3.<sup>43</sup> According to the Routh–Hurwitz criterion, a necessary and sufficient condition for the root of this polynomial to have a negative and non-null real part is (1)  $\alpha > rM_{31}$ , and (2)  $(\alpha - rM_{31})M_{12}M_{21} > \alpha M_{12}M_{21}$ , which is equivalent to  $rM_{31} < 0$  since  $M_{12}$  and  $M_{21}$  are positive, and  $\alpha$  non-negative.

**Appendix B. Heatmap of the Private Debt Ratio**

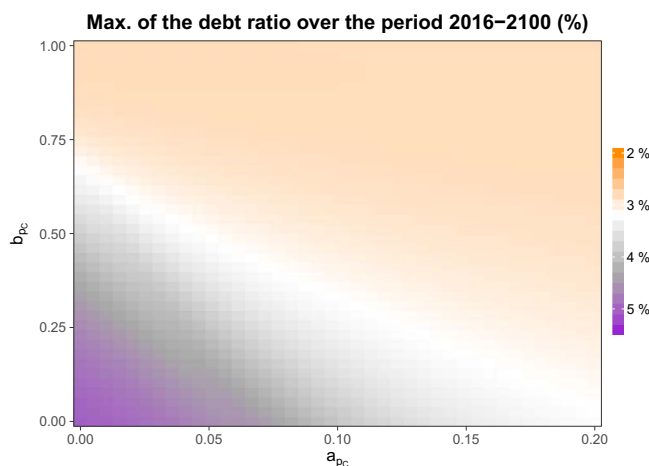


Fig. 10. Heatmaps of the private debt ratio in 2100 in the *Low damage K scenario* with ECS = 3.1.

<sup>43</sup> The latter is similar to the characteristic polynomial found by Grasselli and Lima (2012).

## Appendix C. Calibration of behavioral equations

Three behavioral aggregate functions are calibrated, the investment function,  $\kappa(\cdot)$ , the short-term Phillips curve,  $\Phi(\cdot)$ , and the dividend function,  $\Delta(\cdot)$ . This appendix outlines the methodology followed after introducing the data.

### C.1. The data

The data collection gathers four databases for various time-series:

- World Bank: GDP (current 2010 US\$); Employment-to-population ratio, 15+, total (%) (modeled ILO estimate); Population ages 65 and above (% of total); Population, total and gross fixed capital formation (current US\$);
- Penn World Table: Share of Labor Compensation in GDP at National Prices;
- BIS: Private Debt Non-Financial sector (All sectors, Market value, Percentage of GDP, and Adjusted for breaks);
- FRED St. Louis: Corporate Profits after tax with IVA and CCAadj: Net Dividends, Billions of Dollars, Quarterly, Seasonally Adjusted Annual Rate.

To cope with missing data, as time-series are not available within the same time frame, we selected countries with data available from 1991 to 2014. The list of selected countries includes: Argentina, Australia, Austria, Belgium, Canada, Chile, China, Denmark, Finland, France, Germany, Greece, Hungary, India, Indonesia, Ireland, Israel, Italy, Japan, Malaysia, Mexico, Netherlands, Norway, Portugal, Singapore, South Africa, Spain, Sweden, Switzerland, Thailand, Turkey, the United Kingdom, and the United States.

For simplicity, we assumed a fixed interest rate of 3%. To wrap-up, we were able to retrieve time-series for: the wage growth, the employment rate, the investment-to-GDP ratio, the retained profit rate, and the dividend rate.

### C.2. The methodology

As multinational corporations have become more pervasive, major currency changes have been made (e.g., euro zone), and financial instability has frequently had an impact over the 2000s, it is difficult to find consistency between data in the 1990s and the 2000s. For these reasons, we calibrated the coefficients of the three behavioral function—the investment function,  $\kappa(\cdot)$ , the short-term Phillips curve,  $\Phi(\cdot)$ , and the dividend function,  $\Delta(\cdot)$ —by minimizing the mean square error for data in the aftermath of the burst of the dot-com bubble (i.e. from 2001 on). The calibrated forms are linear. Moreover, it is worth mentioning that for calibration purposes, a fraction of dividend payments has been excluded from the computation of inflation in order to match the initial first moments of the private debt-to-GDP ratio, inflation, and GDP. The values found are the ones reported in [Appendix E](#). More details are available upon request.

## Appendix D. Initial values of the model

Symbol	Description	Value	Remarks and sources
$CO_2^{AT}$	CO <sub>2</sub> -e concentration in the atmosphere layer	851 Gt C	DICE model, <a href="#">Nordhaus (2016)</a>
$CO_2^{UP}$	CO <sub>2</sub> -e concentration in the biosphere and upper ocean layer	460 Gt C	DICE model, <a href="#">Nordhaus (2016)</a>
$CO_2^{LO}$	CO <sub>2</sub> -e concentration in the deeper ocean layer	1740 Gt C	DICE model, <a href="#">Nordhaus (2016)</a>
$d$	Private debt ratio of the economy	1.53	Calibrated, macroeconomic database
$E_{ind}$	Industrial CO <sub>2</sub> -e emissions	35.85 Gt CO <sub>2</sub> -e	DICE model, <a href="#">Nordhaus (2016)</a>
$E_{land}$	Exogenous land use change CO <sub>2</sub> -e emissions	2.6 Gt CO <sub>2</sub> -e	DICE model, <a href="#">Nordhaus (2016)</a>
$F_{exo}$	Exogenous radiative forcing	0.5 W/m <sup>2</sup>	DICE model, <a href="#">Nordhaus (2016)</a>
$g_{\sigma}$	Growth rate of the emission intensity of the economy	- 0.0152	DICE model, <a href="#">Nordhaus (2016)</a>
$p$	Composite good price level	1	Normalization constant
$p_{BS}$	Backstop price level	547.22	DICE model, <a href="#">Nordhaus (2016)</a> , compound 1-year ahead
$n$	Emissions reduction rate	0.03	DICE model, <a href="#">Nordhaus (2016)</a>
$N$	Workforce of the economy in billions	4.83	Calibrated, macroeconomic database
$NG$	Total population in billions	7.35	Calibrated, macroeconomic database
$T$	Temperature in the atmosphere, biosphere and upper ocean layer	0.85 °C	DICE model, <a href="#">Nordhaus (2016)</a>
$T_0$	Temperature in the deeper ocean layer	0.0068 °C	DICE model, <a href="#">Nordhaus (2016)</a>
$Y$	Gross domestic product (at factor prices) in trillions USD	59.74	Calibrated, macroeconomic database
$\lambda$	Employment rate of the economy	0.675	Calibrated, macroeconomic database
$\omega$	Wage share of the economy	0.578	Calibrated, macroeconomic database

## Appendix E. Calibration of the model

Symbol	Description	Value	Remarks and sources
$C$	Heat capacity of the atmosphere, biosphere and upper ocean	1/.098 SI	DICE model, Nordhaus (2016), adjusted for a continuous framework
$C_0$	Heat capacity of the deeper ocean	3.52 SI	DICE model, Nordhaus (2016), adjusted for a continuous framework
$C_{AT_{pind}}$	CO <sub>2</sub> -e preindustrial concentration in the atmosphere layer	588 Gt C	DICE model, Nordhaus (2016)
$C_{UP_{pind}}$	CO <sub>2</sub> -e preindustrial concentration in the biosphere and upper ocean layer	360 Gt C	DICE model, Nordhaus (2016)
$C_{LO_{pind}}$	CO <sub>2</sub> -e preindustrial concentration in the deeper ocean layer	1720 Gt C	DICE model, Nordhaus (2016)
$div_0$	Constant of the dividend function, $\Delta(\cdot)$	0.138	Calibrated, macroeconomic database, more details available upon request
$div_\pi$	Slope of the dividend function, $\Delta(\cdot)$	0.473	Calibrated, macroeconomic database, more details available upon request
$[div_{min}, div_{max}]$	Range of the dividend function, $\Delta(\cdot)$	[0, .3]	Selected among a range of reasonable values
$F_{2 \times CO_2}$	Change in the radiative forcing resulting from a doubling of CO <sub>2</sub> -e concentration w.r.t. to the pre-industrial period	3.681 W/m <sup>2</sup>	DICE model, Nordhaus (2016)
$F_{exo}^{start}$	Initial value of the exogenous radiative forcing	0.5 W/m <sup>2</sup>	DICE model, Nordhaus (2016)
$F_{exo}^{end}$	Value of the exogenous radiative forcing in 2100	1 W/m <sup>2</sup>	DICE model, Nordhaus (2016)
$f_K$	Fraction of environmental damage allocated to the stock of capital	1/3	Dietz and Stern (2015)
$P^N$	Upper limit of the workforce dynamics in billions	7.056	Calibrated, macroeconomic database, more details available upon request
$P_G^N$	Upper limit of the total population dynamics in billions	12	Calibrated, macroeconomic database, more details available upon request
$q$	Speed of growth of the workforce dynamics	0.0305	Calibrated, macroeconomic database, more details available upon request
$q_G$	Speed of growth of the total population dynamics	0.027	Calibrated, macroeconomic database, more details available upon request
$r$	Short-term interest rate of the economy	0.03	Selected among a range of reasonable values
$S$	Equilibrium climate sensitivity	3.1 °C	DICE model, Nordhaus (2016)
$T_{preind}$	Preindustrial temperature	13.74 °C	NASA (2016) NASA (2016)
$\alpha$	Constant growth rate of labor productivity	0.02	Selected among a range of reasonable values
$\gamma^*$	Heat exchange coefficient between temperature layers	0.0176 SI	Nordhaus (2016), adjusted for a continuous framework
$\delta$	Depreciation rate of capital	0.04	Inklaar and Timmer (2013)
$\delta_{E_{land}}$	Growth rate of land use change CO <sub>2</sub> -e emissions	-0.022	DICE model, Nordhaus (2016), adjusted for a continuous framework
$\delta_{g\sigma}$	Variation rate of the growth of emission intensity	-0.001	DICE model, Nordhaus (2016), adjusted for a continuous framework
$\delta_{pBS}$	Exogenous growth rate of the back-stop technology price	-0.005	DICE model, Nordhaus (2016), adjusted for a continuous framework
$\zeta_3$	Damage function parameter	6.754	Weitzman (2011) and Dietz and Stern (2015)
$\eta$	Relaxation parameter of the inflation	0.5	Selected among a range of reasonable values
$\theta$	Parameter of the abatement cost function	2.6	DICE model, Nordhaus (2016)
$\kappa_0$	Constant of the investment function, $\kappa(\cdot)$	0.0318	Calibrated, macroeconomic database, more details available upon request
$\kappa_1$	Slope of the investment function, $\kappa(\cdot)$	0.575	Calibrated, macroeconomic database, more details available upon request
$[\kappa_{min}, \kappa_{max}]$	Range of the investment function, $\kappa(\cdot)$	[0, .3]	Selected among a range of reasonable values
$\mu$	Mark-up of prices over the average cost	1.3	Selected among a range of reasonable values
$\nu$	Constant capital-to-output ratio	2.7	Inklaar and Timmer (2013)
$\pi_1$	Damage function parameter	0/°C	DICE model, Nordhaus (2016), adjusted for a continuous framework
$\pi_2$	Damage function parameter	0.00236/°C <sup>2</sup>	DICE model, Nordhaus (2016)

$\pi_3$	Damage function parameter in the Weitzman case	0.00000507/ °C $\xi_3$	Weitzman (2011) and Dietz and Stern (2015)
$\phi_0$	Constant of short-term Phillips curve, $\phi(\cdot)$	−0.292	Calibrated, macroeconomic database, more details available upon request
$\phi_1$	Slope of the short-term Phillips curve, $\phi(\cdot)$	0.469	Calibrated, macroeconomic database, more details available upon request
$\Phi_{12}$	Transfer coefficient for carbon from the atmosphere to the upper ocean/biosphere	0.024	DICE model, Nordhaus (2016), adjusted for a continuous framework
$\Phi_{23}$	Transfer coefficient for carbon from the upper ocean/biosphere to the lower ocean	0.001	DICE model, Nordhaus (2016), adjusted for a continuous framework

## References

- Akerlof, G.A., Stiglitz, J.E., 1969. Capital, wages and structural unemployment. *Econ. J.* 79 (314), 269–281.
- Barker, T., Anger, A., Chewpreecha, U., Pollitt, H., 2012. A new economics approach to modelling policies to achieve global 2020 targets for climate stabilisation. *Int. Rev. Appl. Econ.* 26, 205–211.
- Barrett, A.B., 2018. Stability of zero-growth economics analysed with a Minskyan model. *Ecol. Econ.* 146 (Supplement C), 228–239.
- Calvo, G.A., 1983. Staggered prices in a utility-maximizing framework. *J. Monet. Econ.* 12 (3), 383–398.
- Carney, M., 2016. Resolving the climate paradox. September 22.
- Carney, M., 2015. Breaking the tragedy of the horizon - climate change and financial stability. September 29.
- Chiarella, C., Di Guilmi, C., 2011, August, August. The financial instability hypothesis: a stochastic microfoundation framework. *J. Econ. Dyn. Control.* 35 (8), 1151–1171.
- Dafermos, Y., Nikolaidi, M., Galanis, G., 2017. A stock-flow-fund ecological macro-economic model. *Ecol. Econ.* 131, 191–207.
- Project, Deep Decarbonization Pathways, 2015. Pathways to deep decarbonization 2015 report.
- Dietz, S., Stern, N., 2015. Endogenous growth, convexity of damage and climate risk: how Nordhaus' framework supports deep cuts in carbon emissions. *Econ. J.* 125 (583), 574–620.
- Dos Santos, C.H., 2005. A stock-flow consistent general framework for formal Minskyan analyses of closed economies. *J. Post Keynesian Econ.* 27 (4), 712–735.
- Fisher, I., 1933. The debt-deflation theory of great depressions. *Econometrica* 1 (4), 337–357.
- Fostel, A., Geanakoplos, J., 2015. Leverage and default in binomial economies: a complete characterization. *Econometrica* 83 (6), 2191–2229.
- Geoffroy, O., Saint-Martin, D., Olivié, D.J.L., Voldoire, A., Bellon, G., Tytéca, S., 2013. Transient climate response in a two-layer energy-balance model. Part I: analytical solution and parameter calibration using CMIP5 AOGCM experiments. *J. Clim.* 26 (6), 1841–1857.
- Gillingham, K., Nordhaus, W.D., Anthoff, D., Blanford, G., Bosetti, V., Christensen, P., McJeon, H., Reilly, J., Sztorc, P., 2015. Modeling Uncertainty in Climate Change: A Multi-model Comparison. Working Paper 21637. National Bureau of Economic Research.
- Giraud, G., 2017. The trouble with climate economics. Comments on “climate change, development, poverty and economics”. In: Fankhauser, S., Stern, N., Basu, K., Rosenblatt, D., Sepulveda, C. (Eds.), *Forthcoming in The State of Economics, The State of the World*. mit press.
- Giraud, G., Grasselli, M.R., 2017. The macrodynamics of household debt, growth, and inequality.
- Godley, W., Lavoie, M., 2012. *Monetary Economics: An Integrated Approach to Credit, Money, Income, Production and Wealth*. Palgrave Macmillan UK.
- Goodwin, R.M., 1967. A growth cycle. In: *Socialism, capitalism and economic growth*. Cambridge University Press, Cambridge, pp. 54–58.
- Grasselli, M., Nguyen-Huu, A., 2015a. Inflation and speculation in a dynamic macro-economic model. *J. Risk Financ. Manag.* 8, 285–310.
- Grasselli, M.R., Costa Lima, B., Wang, X.S., Wu, J., 2014. Destabilizing a stable crisis: employment persistence and government intervention in macroeconomics. *Struct. Chang. Econ. Dyn.* 30, 30–51.
- Grasselli, M.R., Lima, B.C., 2012. An analysis of the Keen model for credit expansion, asset price bubbles and financial fragility. *Math. Finan. Econ.* 6 (3), 191–210.
- Grasselli, M.R., Nguyen-Huu, A., 2015b. Inflation and speculation in a dynamic macro-economic model. *J. Risk Financ. Manag.* 8, 285–310.
- Grasselli, M.R., Nguyen Huu, A., 2018. Inventory growth cycles with debt-financed investment. *Struct. Chang. Econ. Dyn.*
- Hellwig, M.F., 1981. Bankruptcy, limited liability, and the Modigliani–Miller theorem. *Am. Econ. Rev.* 71 (1), 155–170.
- High-Level Commission on Carbon Prices, 2017. Report of the high-level commission on carbon prices. Washington, DC: World Bank. license: Creative commons attribution cc by 3.0 igo.
- Inklaar, R., Timmer, M., 2013. Capital, labor and tfp in pwt8. University of Groningen (unpublished).
- IPCC, 2013. Contribution of Working Group I to the Fifth Assessment Report of the Intergovernmental Panel on Climate Change. In: Stocker, T.F., Qin, D., Plattner, G.-K., Tignor, M., Allen, S.K., Boschung, J., Nauels, A., Xia, Y., Bex, V., Midgley, P.M. (Eds.), *Technical report*. Cambridge University Press, Cambridge, United Kingdom and New York, INY, USA, pp. 1535.
- Jackson, T., 2009. Prosperity Without Growth: Economics for a Finite Planet. Earthscan.
- Keen, S., 1995. Finance and economic breakdown: modeling Minsky's “financial instability hypothesis”. *J. Post Keynesian Econ.* 607–635.
- Lenton, T.M., Held, H., Kriegler, E., Hall, J.W., Lucht, W., Rahmstorf, S., Schellnhuber, H.J., 2008. Tipping elements in the earth's climate system. *Proc. Natl. Acad. Sci.* 23 (6), 1786–1793.
- Mankiw, N., 2010. *Macroeconomics*. Worth Publishers.
- NASA, 2016. Global Station Temperature Index. Link. Accessed: 2016-12-29.
- Nasdaq.com, 2016. Can big oil continue to pay dividends? (February 5). Link Accessed: 2017-07-13.
- Report, New Climate Economy, 2014. Better growth, better climate. Technical report. The Global Commission on the Economy and Climate.
- Nguyen-Huu, A., Costa-Lima, B., 2014. Orbits in a stochastic Goodwin–Lotka–Volterra model. *J. Math. Anal. Appl.* 419 (1), 48–67.
- Nguyen-Huu, A., Pottier, A., 2016. Debt and Investment in the Keen Model: A Reappraisal of Minsky. *Review of Keynesian Economics* 5 (4), 631–647.
- Nordhaus, W., 2016. Projections and uncertainties about climate change in an era of minimal climate policies. *Natl. Bur. Econ. Res. Bull. Aging Health*(w21637).
- Nordhaus, W.D., 1993. Optimal greenhouse-gas reductions and tax policy in the ‘Dice’ model. *Am. Econ. Rev.* 83 (2), 313–317.
- Nordhaus, W.D., 2007. A review of the “stern review on the economics of climate change”. *J. Econ. Lit.* 45 (3), 686–702.
- Nordhaus, W.D., 2014. Estimates of the social cost of carbon: concepts and results from the dice-2013r model and alternative approaches. *J. Assoc. Environ. Resour. Econ.* 1 (1), 273–312.
- Nordhaus, W.D., Sztorc, P., 2013. DICE 2013R: Introduction and User's Manual.
- Rezai, A., Stagl, S., 2016. Ecological macroeconomics: introduction and review. *Ecol. Econ.* 121, 181–185.
- Rezai, A., Taylor, L., Foley, D., 2018. Economic growth, income distribution, and climate change. *Ecol. Econ.* 146 (Supplement C), 164–172.
- Rezai, A., Taylor, L., Mechler, R., 2013. Ecological macroeconomics: an application to climate change. *Ecol. Econ.* 85, 69–76.
- Ryoo, S., 2010. Long waves and short cycles in a model of endogenous financial fragility. *J. Econ. Behav. Organ.* 74 (3), 163–186.
- Schwanitz, V.J., 2013. Evaluating integrated assessment models of global climate change. *Environ. Model. Softw.* 50, 120–131.
- Stanton, E.A., Ackerman, F., Kartha, S., 2009. Inside the integrated assessment models: four issues in climate economics. *Clim. Dev.* 1 (2), 166–184.
- Stern, T.M., Persson, U.M., 2008. An even sterner review: introducing relative prices into the discounting debate. *Rev. Environ. Econ. Policy* 2 (1), 61–76.
- Nations, United, 2015. Department of Economic and Social Affairs, Population Division. *Data Booklet, Population Division. World Population Prospects*.
- Weitzman, M.L., 2011. Fat-tailed uncertainty in the economics of catastrophic climate change. *Rev. Environ. Econ. Policy* 5 (2), 275–292.
- Weitzman, M.L., 2012. Ghg targets as insurance against catastrophic climate damages. *J. Public Econ. Theory* 14 (2), 221–244.